

# Transport Theory beyond Binary Collisions

Margaret E. Carrington

Department of Physics, Brandon University,  
Brandon, Manitoba, R7A 6A9 Canada  
and Winnipeg Institute for Theoretical Physics,  
Winnipeg, Manitoba, Canada

Stanisław Mrowczyński<sup>y</sup>

Soltan Institute for Nuclear Studies,  
ul. Hoża 69, PL - 00-681 Warsaw, Poland  
and Institute of Physics, Świętokrzyska Academy,  
ul. Świętokrzyska 15, PL - 25-406 Kielce, Poland  
(Dated: January 10, 2005)

Using the Schwinger-Keldysh technique, we derive the transport equations for a system of quantum scalar fields. We first discuss the general structure of the equations and then their collision terms. Taking into account up to three-loop diagrams in  $\epsilon^3$  model and up to four-loop diagrams in  $\epsilon^4$  model, we obtain transport equations which include the contributions of multi-particle collisions and particle production processes, in addition to mean-field effects and binary interactions.

PACS numbers: 05.20.Dd, 11.10.Wx

## I. INTRODUCTION

Transport theory is a very convenient tool to study many-body nonequilibrium systems, both relativistic and nonrelativistic. The kinetic equations, which play a central role in the transport approach, usually assume that dissipation processes are governed by binary collisions. However, when the system of interest is very dense one expects that multi-particle interactions will play a significant role. Such interactions are known to the control spectra of fluctuations and transport properties of dense gases and liquids [1]. Furthermore, in relativistic systems a characteristic particle's kinetic energy is usually comparable to the particle's mass, and processes leading to particle production become important for a system's dynamics.

It is therefore expected that multi-particle interactions and production processes will play an important role in the dynamics of a relativistic quark-gluon plasma of high energy density. The importance of gluon multiplication in the process of the plasma's equilibration has been repeatedly stressed, see e.g. [2, 3, 4, 5, 6, 7]. The scattering of three gluons into three gluons has been studied in the context of thermalization in [8]. It has also been shown within the scalar field theory that the transport coefficient of bulk viscosity, as given by the Kubo formula, strongly depends on particle number changing processes [9, 10]. We conclude that a complete description of the quark-gluon plasma based on transport theory requires the derivation of the relativistic transport equation which includes the multi-particle collisions and particle production processes, in addition to the mean-field effects and binary interactions. The form of such an equation has been postulated by some authors, see e.g. [6, 8, 9, 10], but a systematic derivation from first principles is lacking even in the simplest scalar field theory.

The Schwinger-Keldysh [11, 12] formulation of quantum field theory provides a framework for the derivation of the transport equation. Kadano and Baym [13] developed a technique for nonrelativistic quantum systems which has been further generalized to relativistic systems [14, 15, 16, 17, 18, 19, 20, 21, 22, 23, 24]. We mention here only the papers which go beyond the mean-field or Vlasov approximation and provide a more or less systematic analysis of the (binary) collision term.

In this paper, we consider self-interacting scalar fields with cubic and quartic interaction terms and study their transport equations beyond the binary collision approximation. There are basically two separate parts of our study. The first part is the derivation of the general structure of the transport equations. Such an analysis has been published previously by one of us [18, 20, 25] and it is presented here only to provide a framework for the second part of the paper. The main steps of the derivation are the following. We define the contour Green's function with the time arguments

---

<sup>E</sup> Electronic address: carrington@brandonu.ca

<sup>y</sup> Electronic address: mrow@fuw.edu.pl

on the contour in the complex time plane. This function is a key element of the Schwinger-Keldysh approach. After discussing its properties and relevance for nonequilibrium systems, we write down the exact equations of motion i.e. the Dyson-Schwinger equations. We perform a Wigner transformation and do a gradient expansion by assuming that the system has microscopic quasi-homogeneity. The resulting pair of Dyson-Schwinger equations is converted into the transport and mass-shell equations which are satisfied by the Wigner function. We define the distribution function of usual probabilistic interpretation, and we find the transport equations satisfied by this function. The transport equation is derived to lowest order in the gradient expansion, which corresponds to the Markovian limit in which memory terms are neglected.

In the second part of our study, we perform a perturbative analysis of the self-energies which enter the transport equation. We show that the Vlasov or mean-field terms are dominated by the lowest order tadpole diagrams, while binary collisions emerge from two-loop contributions. Multi-particle interactions and production processes appear at three-loop level in the  $^3$  model and at four-loops in the  $^4$  model. There are obviously higher loop contributions to both mean-field and binary collision terms but these higher loop contributions will not change these effects qualitatively, and for this reason are not studied here. Instead we obtain leading order contributions to the collision term that result from  $2 \leftrightarrow 3$  processes in  $^3$  model, and  $2 \leftrightarrow 4$  and  $3 \leftrightarrow 3$  processes in  $^4$  model. To extract the processes represented by the three- and four-loop graphs, we work with the Keldysh representation, using a technique developed previously by one of us [26, 27].

Multi-particle and production processes have already been discussed in the Keldysh-Schwinger approach to transport theory but, to our best knowledge, only for nonrelativistic systems [28, 29, 30]. In this case the analysis is quite different. In the nonrelativistic limit, interactions are instantaneous and internal lines representing the potential interaction cannot be cut. Consequently, the extraction of the scattering matrix elements in the small coupling limit is considerably simpler than in the relativistic case. However, it should be noted that much progress has been achieved in resumming multi-loop diagrams in the nonrelativistic approach [29].

The problem of off-mass-shell transport has recently attracted a lot of attention in the literature [31, 32, 33, 34, 35, 36]. The collision term for off-mass-shell transport contains important contributions from one- and two-loop self-energy diagrams which correspond to  $1 \leftrightarrow 2$  and  $1 \leftrightarrow 3$  processes. These processes are kinematically forbidden for on-mass-shell particles, and for this reason are not studied here.

Throughout this article we use natural units where  $\hbar = c = 1$ . The signature of the metric tensor is  $(+; -; -; -)$ .

## II. PRELIMINARIES

We consider a system of real scalar fields with Lagrangian density of the form

$$\mathcal{L}(\phi) = \frac{1}{2} \partial_\mu \phi(x) \partial^\mu \phi(x) - \frac{1}{2} m^2 \phi^2(x) - \frac{g}{n!} \phi^n(x); \quad (1)$$

where  $n$  equals 3 or 4. The renormalization counterterms are omitted here. The field satisfies the equation of motion

$$(\partial^2 + m^2) \phi(x) = -\frac{g}{(n-1)!} \phi^{n-1}(x); \quad (2)$$

The energy-momentum tensor is defined as

$$T_{\mu\nu}(\phi) = \partial_\mu \phi(x) \partial_\nu \phi(x) - g_{\mu\nu} \mathcal{L}(\phi);$$

Subtracting the total derivative

$$\frac{1}{4} \partial_\mu \partial^\mu \phi^2(x) - g \frac{1}{4} \partial_\mu \partial^\mu \phi^2(x);$$

and considering the case of free fields, we obtain an expression for the energy-momentum tensor which has a form that is convenient for our purposes

$$T_0(\phi) = \frac{1}{4} \phi(x) \partial_\mu \partial^\mu \phi(x); \quad (3)$$

## III. GREEN'S FUNCTIONS

We define the contour Green's function as

$$i(\phi; y) \stackrel{\text{def}}{=} \hbar \Gamma(\phi)(y) i; \quad (4)$$

where  $\langle \dots \rangle$  denotes the ensemble average at time  $t_0$  (usually identified with 1) and  $\mathcal{T}$  is the time ordering operation along the directed contour shown in Fig. 1. The parameter  $t_{\max}$  is shifted to  $+1$  in calculations. The time arguments are complex with an infinitesimal positive or negative imaginary part which locates them on the upper or lower branch of the contour. The ordering operation is defined as

$$\mathcal{T}(x)(y) \stackrel{\text{def}}{=} (x_0; y_0)(x)(y) + (y_0; x_0)(y)(x); \quad (5)$$

where  $(x_0; y_0)$  equals 1 if  $x_0$  succeeds  $y_0$  on the contour, and 0 if  $x_0$  precedes  $y_0$ .

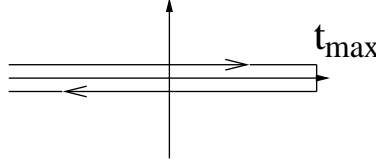


FIG. 1: The contour in the complex time plane for an evaluation of the operator expectation values.

If the field develops a finite expectation value, as is the case when the symmetry is spontaneously broken, the contribution  $\langle x \rangle \langle y \rangle$  is subtracted from the right-hand-side of the equation defining the Green's function and one looks at field fluctuations around the expectation values (see e.g. [18, 20]). Since  $\langle x \rangle$  is expected to vanish in the models defined by the Lagrangians (1) we neglect this contribution in the definition of the Green's function.

The contour propagator involves four functions, which can be thought of as corresponding to propagation along the top branch of the contour, from the top branch to the bottom branch, from the bottom branch to the top branch, and along the bottom branch. Below, we define four Green's functions with real time arguments, and discuss their relationship to the contour Green's function. We define

$$i^>(x; y) \stackrel{\text{def}}{=} \langle x(x) y(y) \rangle; \quad (6)$$

$$i^<(x; y) \stackrel{\text{def}}{=} \langle y(y) x(x) \rangle;$$

$$i^c(x; y) \stackrel{\text{def}}{=} \langle \mathcal{T}^c(x) y(y) \rangle;$$

$$i^a(x; y) \stackrel{\text{def}}{=} \langle \mathcal{T}^a(x) y(y) \rangle;$$

where  $\mathcal{T}^c(\mathcal{T}^a)$  indicates chronological (anti-chronological) time ordering

$$\mathcal{T}^c(x) y(y) \stackrel{\text{def}}{=} (x_0; y_0)(x) y(y) + (y_0; x_0)(y) x(x);$$

$$\mathcal{T}^a(x) y(y) \stackrel{\text{def}}{=} (y_0; x_0)(x) y(y) + (x_0; y_0)(y) x(x);$$

These functions are related to the contour Green's functions in the following manner:

$$i^c(x; y) = \langle x(x) y(y) \rangle \text{ for } x_0; y_0 \text{ on the upper branch;} \quad (7)$$

$$i^a(x; y) = \langle x(x) y(y) \rangle \text{ for } x_0; y_0 \text{ on the lower branch;}$$

$$i^<(x; y) = \langle x(x) y(y) \rangle \text{ for } x_0 \text{ on the upper branch and } y_0 \text{ on the lower one;}$$

$$i^>(x; y) = \langle x(x) y(y) \rangle \text{ for } x_0 \text{ on the lower branch and } y_0 \text{ on the upper one;}$$

The top branch of the contour is usually called the 1' branch and the bottom branch is called the 2' branch. Using this notation, the functions  $i^c$ ,  $i^a$ ,  $i^<$  and  $i^>$  are often written as

$$\begin{aligned} i^c &= \langle 11 \rangle; & i^a &= \langle 22 \rangle; \\ i^< &= \langle 12 \rangle; & i^> &= \langle 21 \rangle; \end{aligned} \quad (8)$$

The following identities can be obtained directly from the definitions given above:

$$\begin{aligned} \hat{G}^a(x; y) &= (x_0 - y_0) \hat{G}^>(x; y) + (y_0 - x_0) \hat{G}^<(x; y); \\ (i \hat{G}^a(x; y))^y &= i \hat{G}^a(x; y) = i \hat{G}^a(y; x); \\ (i \hat{G}^>(x; y))^y &= i \hat{G}^>(x; y) = i \hat{G}^<(y; x); \end{aligned} \quad (9)$$

where the  $y$  denotes hermitian conjugation which involves an interchange of the arguments of the Green's function. Using Eqs. (6) and (9), it is easy to show that the four components of the contour Green's function are not independent but satisfy the relation:

$$\hat{G}^c(x; y) + \hat{G}^a(x; y) - \hat{G}^<(x; y) - \hat{G}^>(x; y) = 0 \quad (10)$$

In some situations, it is useful to work with retarded (+), advanced (−) and symmetric Green's functions. We make the usual definitions for these propagators:

$$i \hat{G}^+(x; y) \stackrel{\text{def}}{=} (x_0 - y_0) h[(x); (y)] i = i (x_0 - y_0) \hat{G}^>(x; y) - \hat{G}^<(x; y); \quad (11)$$

$$i \hat{G}^-(x; y) \stackrel{\text{def}}{=} (y_0 - x_0) h[(x); (y)] i = i (y_0 - x_0) - \hat{G}^<(x; y) + \hat{G}^>(x; y); \quad (12)$$

$$i \hat{G}^{\text{sym}}(x; y) \stackrel{\text{def}}{=} h f[(x); (y)] g i = i \hat{G}^>(x; y) + \hat{G}^<(x; y); \quad (13)$$

where the curly brackets indicate an anticommutator.

It is easy to show that there is a simple relationship between the original set of propagators ( $\hat{G}^c$ ,  $\hat{G}^a$ ,  $\hat{G}^<$  and  $\hat{G}^>$ ) and the retarded, advanced and symmetric propagators ( $\hat{G}^+$ ,  $\hat{G}^-$  and  $\hat{G}^{\text{sym}}$ ). In fact, since the four original propagators satisfy the constraint (10) and thus only three of them are independent, transferring between the two representations is equivalent to a change of basis. Henceforth, we will refer to the set of propagators  $\hat{G}^+$ ,  $\hat{G}^-$  and  $\hat{G}^{\text{sym}}$  as the Keldysh representation of the contour ordered propagator, and the set  $\hat{G}^c$ ,  $\hat{G}^a$ ,  $\hat{G}^<$  and  $\hat{G}^>$  as the 1/2 representation. Using the definitions (6) and the relations (9), it is straightforward to connect the Keldysh to the 1/2 basis

$$\begin{aligned} \hat{G}^c(x; y) &= \hat{G}^c(x; y) - \hat{G}^<(x; y); \\ \hat{G}^>(x; y) &= \frac{1}{2} \hat{G}^{\text{sym}}(x; y) + \hat{G}^+(x; y) - \hat{G}^-(x; y); \\ \hat{G}^+(x; y) - \hat{G}^-(x; y) &= \hat{G}^>(x; y) - \hat{G}^<(x; y); \end{aligned} \quad (14)$$

The relations (9,10,14) hold for real and complex fields. For pure real fields, which are studied here, there are extra relations among Green's functions. In particular, we will make use of the identity

$$\hat{G}^>(x; y) = \hat{G}^<(y; x); \quad (15)$$

We discuss briefly the physical interpretation of the Green's functions we have defined above. The functions  $\hat{G}^a$  and  $\hat{G}^c$  describe the propagation of a disturbance in which a single particle or antiparticle is added to the many-particle system at space-time point  $y$  and then is removed from it at a space-time point  $x$ . The function  $\hat{G}^c(x; y)$  describes a particle disturbance propagating forward in time, and an antiparticle disturbance propagating backward in time. The meaning of  $\hat{G}^a(x; y)$  is analogous but particles are propagated backward in time and antiparticles forward. In the zero density limit  $\hat{G}^c(x; y)$  coincides with the Feynman propagator. In the case of the retarded (advanced) Green functions, both particles and antiparticles evolve forward (backward) in time.

The physical meaning of functions  $\hat{G}^<(x; y)$  is more transparent when one considers their Wigner transforms which are given by

$$\hat{G}^<(X; p) \stackrel{\text{def}}{=} \int d^4 u e^{i p u} \hat{G}^<(X + \frac{1}{2} u; X - \frac{1}{2} u); \quad (16)$$

It is easy to show that the free-field energy-momentum tensor (3) averaged over the ensemble can be expressed as

$$h T_0(X) i = \int \frac{d^4 p}{(2\pi)^4} p_\mu p_\nu i \hat{G}^<(X; p); \quad (17)$$

One recognizes the standard form of the energy-momentum tensor in kinetic theory with the function  $i^{\leq}(X;p)$  playing the role of the density of particles with four-momentum  $p$  at the space-time point  $X$ . This observation leads us to consider  $i^{\leq}(X;p)$  as the quantum analog of the classical distribution function. The function  $i^{\leq}(X;p)$  is hermitian but it is not positive definite, and thus the probabilistic interpretation is only approximately valid. One should also note that, in contrast to the classical distribution function, the function  $i^{\leq}(X;p)$  can be nonzero for the off-mass-shell four-momenta. As will be explicitly shown in Sec. IX, one can extract the usual distribution function from  $i^{\leq}(X;p)$  under specific conditions.

#### IV. EXACT EQUATIONS OF MOTION

Since the Green's function  $i^{\leq}(X;p)$  will be used to obtain the distribution function, we derive an equation which governs the evolution of  $i^{\leq}(X;p)$ . We start with the Dyson-Schwinger equation for the contour Green's function which has the form

$$(x;y) = i_0(x;y) + \int_C^Z d^4 z \int_C^Z d^4 z^0 i_0(x;z) (z;z^0) (z^0;y); \quad (18)$$

where  $i_0(x;y)$  is the free Green's function. We note that the integrals over  $z_0$  and  $z_0^0$  in the last term of equation (18) are performed along the contour.

The Dyson-Schwinger equation (18) can be rewritten as two equations:

$$\partial_x^2 + m^2 (x;y) = i^{(4)}(x;y) + \int_C^Z d^4 x^0 (x;x^0) (x^0;y); \quad (19)$$

$$\partial_y^2 + m^2 (x;y) = i^{(4)}(x;y) + \int_C^Z d^4 x^0 (x;x^0) (x^0;y); \quad (20)$$

where the function  $i^{(4)}(x;y)$  is defined on the contour as

$$i^{(4)}(x;y) = \begin{cases} i^{(4)}(x-y) & \text{for } x_0 > y_0 \text{ from the upper branch;} \\ 0 & \text{for } x_0 < y_0 \text{ from the different branches;} \\ i^{(4)}(x-y) & \text{for } x_0 < y_0 \text{ from the lower branch;} \end{cases}$$

To obtain equations for  $i^{\leq}$  we split the self-energy into three parts as

$$(x;y) = i^{(4)}(x;y) + i^{>}(x;y) (x_0 > y_0) + i^{<}(x;y) (y_0 > x_0); \quad (21)$$

where  $i^{>}$  corresponds to the tadpole contribution to the self-energy. With the help of the retarded and advanced Green's functions (11,12) and similar expressions for the retarded and advanced self-energies, we can rewrite equations (19,20) to obtain

$$\partial_x^2 + m^2 (x) \gtrless (x;y) = \int_C^Z d^4 x^0 \gtrless (x;x^0) (x^0;y) + i^{>}(x;x^0) \gtrless (x^0;y); \quad (22)$$

$$\partial_y^2 + m^2 (y) \gtrless (x;y) = \int_C^Z d^4 x^0 \gtrless (x;x^0) (x^0;y) + i^{>}(x;x^0) \gtrless (x^0;y); \quad (23)$$

where all time integrations run from  $-1$  to  $+1$ .

Similarly, the Dyson-Schwinger equations (19,20) provide the equations satisfied by the retarded and advanced functions  $i^{\lessgtr}(x;y)$  as

$$\partial_x^2 + m^2 (x) \lessgtr (x;y) = i^{(4)}(x-y) + \int_C^Z d^4 x^0 (x;x^0) (x^0;y); \quad (24)$$

$$\partial_y^2 + m^2 (y) \lessgtr (x;y) = i^{(4)}(x-y) + \int_C^Z d^4 x^0 (x;x^0) (x^0;y); \quad (25)$$

We note that the equations for the retarded and for advanced functions are decoupled from each other – there is no mixing of the retarded, advanced and symmetric components of the propagators.

## V. APPROXIMATIONS

It is a very difficult task to study systems which are strongly inhomogeneous or strongly interacting – there are no general methods applicable to such systems. Thus, we assume that systems of interest are weakly inhomogeneous and weakly interacting. We discuss below the mathematical formulation of the corresponding approximations.

1) The system is assumed to be weakly inhomogeneous in comparison with two different length scales.

(a) We assume that the inhomogeneity length is large compared to the inverse of the characteristic momentum i.e.

$$F(X;p) \approx \left(1 - \frac{\partial^2}{\partial X \partial p}\right) F(X;p); \quad (26)$$

where  $F$  is either the propagator or the self-energy. This assumption allows one to perform the gradient expansion.

(b) The inhomogeneity length of the system is assumed to be large compared to the inverse characteristic mass of free quasi-particles (or the Compton wavelength):

$$F(X;p) \approx \left(1 - \frac{1}{m^2} \frac{\partial^2}{\partial X \partial X}\right) F(X;p); \quad (27)$$

This condition justifies the so-called quasi-particle approximation. When the bare fields are massless or the free mass is much smaller than the dynamically generated effective mass  $m$ , the mass in Eq. (27) should be replaced by  $m$  [25].

2) The assumption that the system is weakly interacting means that the coupling constant  $g$  in Eq. (1) is small and that all self-energies can be expanded perturbatively in  $g$ .

The conditions of weak inhomogeneity and weak interaction will be used in two separate ways:

(i) We will convert the equations (22, 23) into transport equations by performing Wigner transformations (16) on all Green's functions and self-energies. Using Eq. (26), we obtain the following set of translation rules:

$$\begin{aligned} \int d^4x^0 f(x;x^0) g(x^0;y) &= f(X;p) g(X;p) + \frac{i}{2} f f(X;p); g(X;p) g; \\ h(x) g(x;y) &= h(X) g(X;p) + \frac{i}{2} \frac{\partial h(X)}{\partial X} \frac{\partial g(X;p)}{\partial p}; \\ h(y) g(x;y) &= h(X) g(X;p) + \frac{i}{2} \frac{\partial h(X)}{\partial X} \frac{\partial g(X;p)}{\partial p}; \\ \partial_x f(x;y) &= \left(-ip + \frac{1}{2} \partial\right) f(X;p); \\ \partial_y f(x;y) &= \left(ip + \frac{1}{2} \partial\right) f(X;p); \end{aligned} \quad (28)$$

where we have introduced the Poisson-like bracket defined as

$$\{C(X;p); D(X;p)\} = \frac{\partial C(X;p)}{\partial p} \frac{\partial D(X;p)}{\partial X} - \frac{\partial C(X;p)}{\partial X} \frac{\partial D(X;p)}{\partial p};$$

The function  $h(x)$  is weakly dependent on  $x$  and we use the notation  $\partial = \frac{\partial}{\partial x}$ . This calculation is done in Sec. VI.

(ii) The condition (27) allows one to drop the terms containing  $\partial^2$ . These terms and those involving  $\text{Im} \tau^+$ , which are discussed in (iv), are responsible for off-mass-shell contributions to the Green's functions  $\hat{G}^{\pm}$ .

(iii) The assumption (26) is used together with the condition of weak interaction to show that the gradient terms in the right hand side of the transport equation (35) and mass-shell equation (36) can be dropped. This point is discussed in detail in Sec. VI.

(iv) The weakly interacting approximation is used in Sec. X. For  $l=g=1$  and a finite bare mass, we have

$$m^2 = \text{Re } \Sigma + i\text{Im } \Sigma; \quad (29)$$

This assumption combined with the condition (27) allows us to obtain an expression for the spectral function that is proportional to  $(p^2 - m^2)$ . We note that both of equations (27) and (29) are commonly called 'the quasiparticle approximation'. This terminology is a consequence of the fact that there are two independent means by which the quasiparticle picture can be destroyed: strong inhomogeneity and strong interactions.

(v) The weakly interacting condition is also used in Sec. XII to perform a perturbative expansion of the self-energies in the collision term of the transport equation. Each term in this expansion represents a different physical contribution to the transport equation.

## VI. EQUATIONS FOR $\hat{G}$

Applying the translation rules (28) to Eqs. (22, 23), neglecting the term proportional to  $\partial^2$  due to the quasiparticle approximation (27), and taking the difference and sum of the equations, we obtain

$$\begin{aligned} \hbar \partial_p \partial_{\vec{p}} \frac{1}{2} \partial_{\vec{p}} (\hat{X}) \hat{G}_p^i(\vec{X}; p) &= \frac{i}{2} \left[ \hat{G}^>(\vec{X}; p) - \hat{G}^<(\vec{X}; p) - \hat{G}^<(\vec{X}; p) + \hat{G}^>(\vec{X}; p) \right. \\ &\quad \left. - \frac{1}{4} \hat{G}^>(\vec{X}; p); \hat{G}^<(\vec{X}; p) + \hat{G}^<(\vec{X}; p) \right] \\ &\quad \left. + \frac{1}{4} \hat{G}^>(\vec{X}; p) + \hat{G}^<(\vec{X}; p); \hat{G}^>(\vec{X}; p) \right]; \end{aligned} \quad (30)$$

$$\begin{aligned} \hbar \frac{p^2 + m^2}{2} \hat{G}_p^i(\vec{X}; p) &= \frac{1}{2} \left[ \hat{G}^>(\vec{X}; p) + \hat{G}^<(\vec{X}; p) + \hat{G}^<(\vec{X}; p) + \hat{G}^>(\vec{X}; p) + \hat{G}^<(\vec{X}; p) \right] \hat{G}^>(\vec{X}; p) \\ &\quad + \frac{i}{4} \hat{G}^>(\vec{X}; p); \hat{G}^<(\vec{X}; p) - \frac{i}{4} \hat{G}^<(\vec{X}; p); \hat{G}^>(\vec{X}; p) \right]; \end{aligned} \quad (31)$$

where we have used the identity (14) applied to the Green's functions and self-energies. One recognizes Eq. (30) as a transport equation while Eq. (31) is called a mass-shell equation. We note that in the limit of free fields, Eqs. (30, 31) become

$$\partial_p \partial_{\vec{p}} \hat{G}_0^i(\vec{X}; p) = 0; \quad (32)$$

$$p^2 - m^2 \hat{G}_0^i(\vec{X}; p) = 0; \quad (33)$$

Due to Eq. (33),  $\hat{G}_0^i(\vec{X}; p)$  is proportional to  $(p^2 - m^2)$ , and consequently free quasiparticles are always on mass-shell. We note that if the quasiparticle approximation (27) were not used, the mass-shell equation would have the form

$$\frac{\hbar}{4} \partial^2 \frac{1}{p^2 + m^2} \hat{G}_0^i(\vec{X}; p) = 0; \quad (34)$$

and the on-shell contribution to the Green's function  $\hat{G}_0^i$  would be nonzero.

The equations (30, 31) can be rewritten in a more compact way:

$$\begin{aligned} \hbar \frac{p^2 - m^2}{2} \hat{G}_p^i(\vec{X}; p) + \text{Re } \Sigma(\vec{X}; p) \hat{G}_p^i(\vec{X}; p) &= \frac{i}{2} \left[ \hat{G}^>(\vec{X}; p) - \hat{G}^<(\vec{X}; p) - \hat{G}^<(\vec{X}; p) + \hat{G}^>(\vec{X}; p) \right. \\ &\quad \left. - \frac{1}{4} \hat{G}^>(\vec{X}; p); \hat{G}^<(\vec{X}; p) + \hat{G}^<(\vec{X}; p) \right] \hat{G}_p^i(\vec{X}; p) \end{aligned} \quad (35)$$

$$\begin{aligned} \hbar \frac{p^2 - m^2}{2} \hat{G}_p^i(\vec{X}; p) + \text{Re } \Sigma(\vec{X}; p) \hat{G}_p^i(\vec{X}; p) &= \hat{G}_p^i(\vec{X}; p) \text{Re } \Sigma(\vec{X}; p) \\ &\quad + \frac{i}{4} \hat{G}^>(\vec{X}; p); \hat{G}^<(\vec{X}; p) + \frac{i}{4} \hat{G}^<(\vec{X}; p); \hat{G}^>(\vec{X}; p); \end{aligned} \quad (36)$$

where

$$\text{Re } (\chi; p) = \frac{1}{2} + (\chi; p) + (\chi; p); \quad \text{Im } (\chi; p) = \frac{1}{2i} + (\chi; p) (\chi; p) : \quad (37)$$

We note that  $i (\chi; p)^y = i (\chi; p)$  which is a direct consequence of the definitions (11,12). The equation analogous to Eq. (35) was earlier derived in [13, 14, 25].

The gradient terms in the right-hand-sides of Eqs. (35,36) are usually neglected. The justification for dropping these terms is considered below. The small parameter that characterizes the gradient expansion will be denoted  $\epsilon$ . In Sec. XII we will calculate the selfenergies using a perturbative expansion in the coupling constant  $g$ . For the purposes of the discussion below, we will use a new parameter to characterize the coupling constant expansion. This new parameter is defined by  $\epsilon = g$  for  $^3$  and  $\epsilon = \sqrt{g}$  for  $^4$  theory. The parameter  $\epsilon$  is introduced to simplify the notation: the leading order contributions to  $(\chi) + \text{Re } ^+(\chi; p)$  and  $^z(\chi; p)$  are of order  $\epsilon^2$  and  $\epsilon^4$  respectively, in both  $^3$  and  $^4$  theory [43].

Now, we compute the order of each term in Eq. (35). We can split the Poisson-like bracket on the left hand side into two pieces. The first piece does not contain the self-energy and is of order  $\epsilon^2$ . The second piece is of order  $\epsilon^2$ . The first term on the right hand side (the term without the Poisson-like bracket) is of order  $\epsilon^4$ , and the term with the Poisson-bracket (the gradient term) is of order  $\epsilon^4$ . Thus, we find that the gradient term on the right hand side of Eq. (35) is of higher order than the remaining terms and can be dropped. Similarly, the gradient term on the right hand side of Eq. (36) is of order  $\epsilon^4$  and it is of higher order than the remaining terms.

We note that the argument presented above breaks down close to equilibrium. At equilibrium the non-gradient term on the right hand side of Eq. (35) is identically zero, and thus cannot be considered to be bigger than the gradient term. In the equilibrium case, it has been shown that the gradient term does not need to be dropped but can be combined with the interaction term on the left hand side to produce the usual Vlasov term [25]. The very-close-to-equilibrium situation is not fully understood.

## VII. EQUATIONS FOR

We also write down the transport and mass-shell equations satisfied by the retarded and advanced Green's functions. Starting with Eqs. (24,25), one finds

$$p^2 - m^2 + (\chi) + (\chi; p); \quad (\chi; p)^o = 0; \quad (38)$$

$$p^2 - m^2 + (\chi) + (\chi; p)^i (\chi; p) = 1; \quad (39)$$

We observe that the gradient terms drop out entirely in Eq. (39). The leading order corrections to this equation are second order in the gradient expansion. Equation (39) can be immediately solved to give

$$(\chi; p) = \frac{1}{p^2 - m^2 + (\chi) + (\chi; p)}; \quad (40)$$

We note that any function  $f(K)$  satisfies the equation  $f(K); f(K)g = 0$ , for  $K$  an arbitrary function of  $X$  and  $p$ . Thus, the expression (40) solves Eq. (38) as well as Eq. (39).

The real and imaginary parts of  $(\chi; p)$ , which we will need later, are

$$\text{Re } (\chi; p) = \frac{p^2 - m^2 + (\chi) + \text{Re } ^+(\chi; p)}{p^2 - m^2 + (\chi) + \text{Re } ^+(\chi; p)^2 + \text{Im } ^+(\chi; p)^2}; \quad (41)$$

$$\text{Im } (\chi; p) = \frac{\text{Im } ^+(\chi; p)}{p^2 - m^2 + (\chi) + \text{Re } ^+(\chi; p)^2 + \text{Im } ^+(\chi; p)^2}; \quad (42)$$

Using the relations (11,12), we can obtain the Wigner transforms of the retarded and advanced functions for free fields

$$(\chi; p)^o = \frac{1}{p^2 - m^2 - ip0^+}; \quad (43)$$

Comparing the expressions (40) and (43), we find that in the limit  $g \rightarrow 0$  the selfenergies must satisfy

$$\text{Im } ^+(\chi; p) = \text{Im } (\chi; p) = \begin{cases} 0^+ & \text{for } p_0 > 0; \\ 0 & \text{for } p_0 < 0; \end{cases} \quad (44)$$



## V III. S P E C T R A L F U N C T I O N

In this section, we introduce another function which will be useful later on. The spectral function  $A$  is defined as

$$A(x; y) \stackrel{\text{def}}{=} h[x(y)] = i^{-1} \langle x; y \rangle - i^{-1} \langle x; y \rangle = i^{-1} \langle x; y \rangle - i^{-1} \langle x; y \rangle = 2 \text{Im} \langle x; y \rangle; \quad (45)$$

where  $[x(y)]$  denotes the field commutator. For real fields, which are studied here,  $A(X; p) = A(X; -p)$ .

From the transport and mass-shell equations (35, 36), one immediately finds equations for  $A(X; p)$  of the form

$$p^2 - m^2 + \langle X \rangle + \text{Re} \langle X; p \rangle; A(X; p) = 2 \text{Im} \langle X; p \rangle; \text{Re} \langle X; p \rangle; \quad (46)$$

$$p^2 - m^2 + \langle X \rangle + \text{Re} \langle X; p \rangle A(X; p) = 2 \text{Im} \langle X; p \rangle \text{Re} \langle X; p \rangle; \quad (47)$$

Substituting the formula (41) into the algebraic equation (47), we find the solution

$$A(X; p) = \frac{2 \text{Im} \langle X; p \rangle}{p^2 - m^2 + \langle X \rangle + \text{Re} \langle X; p \rangle^2 + \text{Im} \langle X; p \rangle^2}; \quad (48)$$

It is easy to show that the function (48) solves Eq. (46) as well. In fact, the spectral function (48) can be found directly from Eq (42) due to the last equality in Eq. (45).

The free spectral function can be obtained from the free retarded and advanced functions (43) by means of the relation (45). It can be also found from Eq. (48) using the condition (44). In either case one needs to make use of the well-known identity

$$\frac{1}{x - i0} = P \frac{1}{x} - i \pi \delta(x); \quad (49)$$

We obtain

$$A_0(X; p) = 2 \langle p^2 - m^2 \rangle (p_0) \delta(p_0); \quad (50)$$

When  $\text{Im} \langle X; p \rangle = 0$  the spectral function describes infinitely narrow quasi-particles with energies uniquely determined by their momenta. When  $\text{Im} \langle X; p \rangle \neq 0$  the quasi-particles are of finite life time, and the spectral function gives the energy distribution of a quasi-particle with a given momentum.

## IX. D I S T R I B U T I O N F U N C T I O N

The distribution function  $f(X; p)$  is defined through the equation

$$(p_0) A(X; p) f(X; p) \stackrel{\text{def}}{=} (p_0) i^{-1} \langle X; p \rangle; \quad (51)$$

where  $A(X; p)$  is the spectral function (48). This definition is motivated by Eq. (17) which leads us to identify  $i^{-1} \langle X; p \rangle$  as the quantum analogue of the classical distribution function. We note that  $f(X; p)$  depends not on the three-vector  $p$  but on the four-vector  $p$ . Using Eq. (45) and the identity (15) in the form  $i^{-1} \langle X; p \rangle = i^{-1} \langle X; -p \rangle$ , we have

$$i^{-1} \langle X; p \rangle = (p_0) A(X; p) f(X; p) + 1 - (p_0) A(X; p) f(X; -p); \quad (52)$$

$$i^{-1} \langle X; p \rangle = (p_0) A(X; p) f(X; p) - (p_0) A(X; p) f(X; -p) + 1; \quad (53)$$

In the case of free fields, Eqs. (52, 53) simplify to

$$i^{-1} \langle X; p \rangle = 2 \langle p^2 - m^2 \rangle (p_0) f_0(X; p) + 1 + (p_0) f_0(X; -p) \quad (54)$$

$$= \frac{1}{E_p} (E_p - p_0) f_0(X; p) + 1 + \frac{1}{E_p} (E_p + p_0) f_0(X; -p);$$

$$i^{-1} \langle X; p \rangle = 2 \langle p^2 - m^2 \rangle (p_0) f_0(X; p) + (p_0) f_0(X; -p) + 1 \quad (55)$$

$$= \frac{1}{E_p} (E_p - p_0) f_0(X; p) + \frac{1}{E_p} (E_p + p_0) f_0(X; -p) + 1;$$

where the explicit form of the free spectral function (50) was used.

For future use, we write down the results for the propagators  $\epsilon_0$ ,  $a_0$  and  $\epsilon_0^{\text{sym}}$  in terms of the free distribution function  $f_0$ . Using the free retarded and advanced functions (43) and the identity (49), we obtain

$$\begin{aligned} i \epsilon_0^>(X;p) &= i \epsilon_0^+(X;p) + i \epsilon_0^<(X;p) \\ &= \frac{i}{p^2 - m^2 + i0^+} + 2 \int \frac{d^3k}{(2\pi)^3 2E_k} (p_0 - k_0) f_0(X;p) + \int \frac{d^3k}{(2\pi)^3 2E_k} (p_0 + k_0) f_0(X;p) \end{aligned} \quad (56)$$

$$\begin{aligned} i \epsilon_0^a(X;p) &= i \epsilon_0^-(X;p) + i \epsilon_0^<(X;p) \\ &= \frac{i}{p^2 - m^2 - i0^+} + 2 \int \frac{d^3k}{(2\pi)^3 2E_k} (p_0 - k_0) f_0(X;p) + \int \frac{d^3k}{(2\pi)^3 2E_k} (p_0 + k_0) f_0(X;p); \end{aligned} \quad (57)$$

$$\begin{aligned} i \epsilon_0^{\text{sym}}(X;p) &= i \epsilon_0^>(X;p) + i \epsilon_0^<(X;p) \\ &= 2 \int \frac{d^3k}{(2\pi)^3 2E_k} (p_0 - k_0) f_0(X;p) + 2 \int \frac{d^3k}{(2\pi)^3 2E_k} (p_0 + k_0) f_0(X;p) + 1; \end{aligned} \quad (58)$$

We note that in the case of equilibrium (homogeneous) systems, the familiar definition of the distribution function is

$$f^{\text{eq}}(p) \stackrel{\text{def}}{=} \frac{1}{V} \langle a^\dagger(p) a(p) \rangle; \quad (59)$$

where  $V$  denotes the system volume and  $a(p)$  and  $a^\dagger(p)$  are annihilation and creation operators, respectively. The definition (51) should reduce to (59) when an equilibrium (homogeneous) system is considered. We discuss this point below for the case of a noninteracting system for which the field that solves the equation of motion (2) can be written as

$$\phi(x) = \int \frac{d^3k}{(2\pi)^3 2E_k} e^{ikx} a(k) + e^{ikx} a^\dagger(k); \quad (60)$$

where  $k = (E_k; \mathbf{k})$ . Substituting the solution (60) into the definition (6) one finds

$$\begin{aligned} i \epsilon_0^>(X;p) &= \int \frac{d^3k}{(2\pi)^3 2E_k} \int \frac{d^3q}{(2\pi)^3 2E_q} (2\pi)^4 \\ &\quad \int_0^h e^{i(k+q)X} \left( p - \frac{k+q}{2} \right) \langle a(k) a(q) \rangle + e^{i(k-q)X} \left( p - \frac{k+q}{2} \right) \langle a(k) a^\dagger(q) \rangle \\ &\quad + e^{i(k-q)X} \left( p + \frac{k+q}{2} \right) \langle a^\dagger(k) a(q) \rangle + e^{i(k+q)X} \left( p + \frac{k+q}{2} \right) \langle a^\dagger(k) a^\dagger(q) \rangle; \end{aligned} \quad (61)$$

Since we restrict ourselves to the consideration of homogeneous systems, we require that the function  $\epsilon_0^>(X;p)$  is independent of  $X$ . One ansatz that satisfies this constraint is given by

$$\langle a(k) a(q) \rangle = 0; \quad \langle a^\dagger(k) a^\dagger(q) \rangle = 0; \quad (62)$$

and

$$\langle a(k) a^\dagger(q) \rangle = \frac{(3)(k-q)}{V} \langle a(k) a^\dagger(k) \rangle; \quad \langle a^\dagger(k) a(q) \rangle = \frac{(3)(k-q)}{V} \langle a^\dagger(k) a(k) \rangle; \quad (63)$$

Using these expressions, the integrals in Eq. (61) are trivially performed and we obtain

$$i \epsilon_0^>(p) = \frac{1}{E_p} (E_p - p_0) \frac{1}{V} \langle a(p) a^\dagger(p) \rangle + \frac{1}{E_p} (E_p + p_0) \frac{1}{V} \langle a^\dagger(p) a(p) \rangle; \quad (64)$$

Using the commutation relation  $[a(p); a^\dagger(k)] = (3)(p-k)$ , which gives

$$\langle a(k) a^\dagger(k) \rangle = \langle a^\dagger(k) a(k) \rangle + V;$$

one finds that Eq. (64) combined with the definition (59) reproduces (55). Thus we have shown that the definitions (51) and (59) are consistent with each other for homogeneous systems. One notes that for nonhomogeneous systems the conditions (62,63) are, in principle, not fulfilled. As a result, the functions  $\epsilon_0^>(X;p)$  are not only  $X$ -dependent but also have support for on-shell momenta in agreement with Eq. (34). Therefore, the expressions (54,55) can be treated as a representation of  $\epsilon_0^>(X;p)$  only for weakly nonhomogeneous systems.

## X. MASS-SHELL CONSTRAINT

In this section we discuss two issues that are related to the mass shell constraint. We first show that in the homogeneous limit (or neglecting gradient terms), the mass shell condition is satisfied if the distribution function is defined in terms of the spectral function as in Eq. (51), and if this distribution function satisfies the transport equation. Secondly, we show that using this definition of the distribution function, the mass-shell constraint reduces to the familiar definition of the mass-shell condition on the four-momentum in the limit of zero width quasi-particles.

The transport and mass-shell equations for a homogeneous system, which are obtained from Eqs. (35) and (36) by dropping gradient terms, read

$$\partial_t \langle X; p \rangle - \partial_i \langle X; p \rangle \partial_i \langle X; p \rangle + \langle X; p \rangle \partial_i \langle X; p \rangle = 0; \quad (65)$$

$$p^2 - m^2 + \langle X \rangle + \text{Re} \partial_i \langle X; p \rangle \partial_i \langle X; p \rangle = \partial_i \langle X; p \rangle \text{Re} \partial_i \langle X; p \rangle : \quad (66)$$

These equations can be rewritten using Eqs. (52,53) which express  $\langle X; p \rangle$  through the distribution function. We work below with the mass-shell equation for  $\langle X; p \rangle$  and restrict to  $p_0 > 0$ . It is straightforward to repeat all steps with  $p_0 < 0$ , and for  $\langle X \rangle$  with  $p_0 > 0$  and  $p_0 < 0$ . We find

$$A \langle X; p \rangle \partial_t \langle X; p \rangle f \langle X; p \rangle - \partial_i \langle X; p \rangle f \langle X; p \rangle + 1 = 0; \quad (67)$$

$$p^2 - m^2 + \langle X \rangle + \text{Re} \partial_i \langle X; p \rangle A \langle X; p \rangle f \langle X; p \rangle = \partial_i \langle X; p \rangle \text{Re} \partial_i \langle X; p \rangle : \quad (68)$$

Using the spectral function equation (47), the mass-shell equation (68) has the form

$$\text{Re} \partial_i \langle X; p \rangle \partial_i \langle X; p \rangle f \langle X; p \rangle - \partial_i \langle X; p \rangle f \langle X; p \rangle + 1 = 0 : \quad (69)$$

One sees that if  $f$  solves Eq. (67), it automatically satisfies Eq. (69). Equivalently, the transport and mass-shell equations (35) and (36) can be replaced with the two equations (47) and (67) in the homogeneous limit.

We note that the equations (67, 68), which were obtained by neglecting gradient terms, are exact for equilibrium (homogeneous) systems. These equations can be written as

$$\partial_t f^{\text{eq}}(p) = \partial_i f^{\text{eq}}(p) \partial_i f^{\text{eq}}(p) + 1; \quad (70)$$

which is the well-known Kubo-Martin-Schwinger (KMS) condition, see e.g. [13], that is satisfied by the self-energy in equilibrium. We also note that in going from equations (35) and (36) to equations (47) and (67), we have replaced four equations with two. This reduction in the number of independent Green's functions is expected since in equilibrium the two functions  $\partial_i \langle X; p \rangle$  are not independent but related through a KMS condition of the form (70).

We have shown above that when the distribution function is defined by Eq. (51), the transport and mass-shell equations (35,36) can be replaced by the equations (47) and (67). In the limit  $\text{Im} \partial_i \langle X; p \rangle \rightarrow 0$  the solution to Eq. (47), which is given by Eq. (48), becomes

$$A \langle X; p \rangle = 2 \left( (p_0) - (p_0) \right) (p^2 - m^2 + \langle X \rangle + \text{Re} \partial_i \langle X; p \rangle) : \quad (71)$$

The argument of the delta function gives the usual form of the mass-shell constraint of the four-momentum

$$p^2 - m^2 + \langle X \rangle + \text{Re} \partial_i \langle X; p \rangle = 0; \quad (72)$$

which tell us that only three out of four momentum components are independent. For  $\text{Im} \partial_i \langle X; p \rangle$  small but finite, this equation determines the position of the maximum of the spectral function.

We note that when the system of interest is significantly inhomogeneous, cf. Eq. (34), or when an interaction generates a non-negligible value of  $\text{Im} \partial_i \langle X; p \rangle$ , the function  $\partial_i \langle X; p \rangle$ , which solves Eq. (36), has support from momenta not satisfying the relation (72). In this case, one has finite-width quasi-particles and the equation (72) only gives, according to Eq. (48), the most probable energy of a quasi-particle. Thus, the statement that the four-momentum is on the mass-shell (72) and the statement that the function  $\partial_i \langle X; p \rangle$  satisfies the mass-shell constraint (36) are, in general, not equivalent.

## X I. T R A N S P O R T E Q U A T I O N

The distribution function  $f$  satisfies the transport equation which can be obtained from Eq. (35) for  $>$  or  $<$ . Using Eqs. (46) and (51), one finds

$$\begin{aligned} (p_0) A(X;p) p^2 - m^2 + (X) + \text{Re}^+ (X;p); f(X;p) \\ = i (p_0) A(X;p) > (X;p) f(X;p) < (X;p) f(X;p) + 1 \\ + f(X;p) > (X;p); \text{Re}^+ (X;p) \\ f(X;p) + 1 < (X;p); \text{Re}^+ (X;p) ; \end{aligned} \quad (73)$$

where we have used the identity

$$A; B C = A; B C + A; C B :$$

Neglecting the gradient terms in the r.h.s. of Eq. (73), we obtain the equation

$$(p_0) p^2 - m^2 + (X) + \text{Re}^+ (X;p); f(X;p) = i (p_0) > (X;p) f(X;p) < (X;p) f(X;p) + 1 : \quad (74)$$

The transport equation (74) greatly simplifies for zero-width quasi-particles. Using the mass-shell condition (72), and taking the positive energy solution, one can evaluate the Poisson-like bracket to obtain

$$(p_0) p^2 - m^2 + (X) + \text{Re}^+ (X;p); f(X;p) = 2E_p \frac{\partial}{\partial t} + v \cdot r f(X;p) + 2r \cdot V(X;p) r_p f(X;p) ; \quad (75)$$

where

$$V(X;p) = (X) + \text{Re}^+ (X;p) ;$$

and the velocity  $v = \partial E_p / \partial p$ . Note that  $E_p$  is not  $\sqrt{p^2 + m^2}$  but the positive solution of Eq. (72). Substituting Eq. (75) into Eq. (74), the transport equation takes the form

$$E_p \frac{\partial}{\partial t} + v \cdot r f(X;p) + r \cdot V(X;p) r_p f(X;p) = (p_0) \frac{1}{2} > (X;p) f(X;p) < (X;p) f(X;p) + 1 : \quad (76)$$

In the left hand side of Eq. (76), one recognizes the standard drift and Vlasov terms [37]. The calculation of the self-energies  $\text{Re}^+$  and  $\text{Im}$  in the Vlasov term is straightforward and the physical interpretation is well known: they contribute to mean field effects and result in the generation of an effective mass. In this paper we will not discuss these terms (they have been studied in detail in [18]). From the right hand side of Eq. (76), one defines the collision term  $C(X;p)$  as

$$(p_0) C(X;p) \stackrel{\text{def}}{=} (p_0) \frac{1}{2} > (X;p) f(X;p) < (X;p) f(X;p) + 1 : \quad (77)$$

The structure of this collision term is the subject of the next few sections.

## X I I. C O L L I S I O N T E R M S T R U C T U R E

In order to obtain physical results from the transport equation derived in the previous sections, we must specify the self-energies that appear in the collision term. We will assume that the interaction is sufficiently weak that the self-energies can be expanded in powers of the coupling constant, and thus expressed through the Green's functions. We will develop a diagrammatic expansion of the self-energies and identify the different physical processes that contribute to the collision term (77). The collision terms we obtain are local in space-time, and consequently valid in the Markovian limit where all memory effects are neglected.

We first rewrite Eq. (77) by multiplying by the spectral function  $A(X;p)$  and using Eq. (51). Thus, we obtain the equation

$$(p_0) A(X;p) C(X;p) = (p_0) \frac{1}{2} < (X;p) > (X;p) > (X;p) < (X;p) : \quad (78)$$

Evolution along the contour illustrated in Fig. 1 is formally very similar to evolution along the real time axis, and consequently it is possible to develop perturbation theory on the contour. Self-energies with real time arguments, in particular  $\Sigma^<$ , have to be extracted from the contour self-energy. Since these calculations involve summations over contributions from both branches of the contour, they are much more difficult than their vacuum counterparts. There are several different methods that can be used which are based on different representations of real time field theory [38] and each has its advantages and proponents. At the lower loop levels, the relevant self-energies have been calculated in several different ways both in equilibrium [39] and non-equilibrium [18]. (A general structure of the equilibrium self-energy expressed through the scattering amplitude has been studied in [40].) At three or more loops, the calculation is extremely cumbersome and requires the use of special methods.

Our calculation of the self-energies, which enter the collision term of transport equation, uses the Keldysh representation formulated in terms of retarded, advanced and symmetric Green functions. To understand why the Keldysh representation is better suited to perform such a calculation, we need to look at the Wigner transformed propagators for non-interacting fields in the Keldysh and 1/2 representation. In the 1/2 basis the propagators are given by equations (54, 55, 56, 57) and in the Keldysh basis by (43, 58). The functions  $i_0^<$  and  $i_0^>$  do not contain on-mass-shell contributions that have the form of propagators. They are non-zero only on the mass-shell. In contrast,  $i_0^<$  and  $i_0^>$  contain one piece that corresponds to time-ordered and anti-time-ordered propagation, respectively, and one piece that is non-zero only on the mass shell. In the Keldysh basis, however, none of the Green's functions mixes the propagating pieces and terms that are non-zero only on the mass-shell:  $G_0^+$  and  $G_0^-$  contain only the contributions corresponding to retarded and advanced propagation, respectively, and  $G_0^{\text{sym}}$  is non-zero only on-mass-shell. Remembering that on-mass-shell Green functions represent real particles and propagating Green functions virtual particles, it is not unexpected that this clean separation of real and virtual particles makes the physical interpretation of the collision term much more straightforward.

We switch to the Keldysh basis using the relations (14) and analogous relations for the self-energies. The collision term (78), which will be computed in the next sections up to four-loop level, then equals

$$(p_0)A(p)C(p) = \frac{1}{4} (p_0)^h (p_0)^{\text{sym}}(p) + (p_0)^h (p_0)^h + (p_0)^h (p_0)^{\text{sym}}(p) : \quad (79)$$

It will be shown that in the Keldysh representation, all contributions to the collision term have the form of 'cuts' [27]. We use the word 'cut' in the way that it is usually used when discussing the calculation of the imaginary part of a diagram: a 'cut line' passes through a diagram from top to bottom dividing it into two parts, so that each part contains at least one external leg. A propagator that is crossed by the cut line becomes a 'cut propagator' which means that it has been put on the mass shell.

We introduce the notion 'central cut' to refer to the cut for which all loops contain at least one cut propagator. For the one-loop diagram in  $^3$  theory, and the two-loop diagram in  $^4$  theory, the only possible cut is the central cut. At two and more loops in  $^3$  theory, and three and more loops in  $^4$  theory, all diagrams contain contributions from non-central cuts. In addition, there are some diagrams for which no central cut exists. In each case however, the contributions from non-central cuts can be included as renormalized lower loop terms. An example of this is presented in Sec. X IV B. The main thrust of our paper involves the analysis of the central cuts of three- and four-loop diagrams.

The calculation of a self-energy graph involves two non-trivial steps: the calculation of the integrand and the computation of the integral itself. In this paper we are primarily interested in the calculation of integrands which determine the structure of the collision term. At three or more loops, calculating by hand in any representation is extremely tedious. We use a MATHEMATICA program developed by one of us, which is described in detail in [26], to calculate the integrand. To use the program one assigns momenta and indices to every line and vertex in the diagram. Each index can take the values 1 or 2, corresponding to the top and bottom branches of the contour. The indices that correspond to external legs take fixed values, and a specific combination corresponds to a specific self-energy in the 1/2 representation, in analogy with Eq. (8). Internal indices are summed over their two possible values 1 and 2. Using Eqs. (8,13,14), one switches to the Keldysh representation. A huge number of terms is produced even for fairly simple diagrams. However, there are many cancellations between these terms. The program identifies the surviving contributions and provides them as output.

In Secs. X III and X IV we rederive the well known one- and two-loop results to illustrate our technique. In Sec. X V we use our method to obtain results for three-loop diagrams which contribute to  $2 \rightarrow 3$  processes in  $^3$  theory, and in Sec. X VI we study four-loop diagrams in  $^4$  theory which correspond to  $2 \rightarrow 4$  and  $3 \rightarrow 3$  processes.

## X III. ONE-LOOP CONTRIBUTIONS

We start by considering the lowest order contributions. In the  $^4$  model, the only one-loop diagram is the tadpole. It is well known that this diagram only contributes to mean-field dynamics, see e.g. [18], and therefore it will not be discussed here. For  $^3$  theory, the one-loop contribution to the self-energy, which is shown in Fig. 2, has a non-trivial imaginary part. The related scattering amplitude corresponds to  $1 \rightarrow 2$  processes which are kinematically forbidden for on-shell particles, as an on-shell particle of mass  $m$  cannot decay into two on-shell particles with the same masses. However, it is important to remember that the process is allowed for virtual particles and has been repeatedly discussed, in particular, in the context of electron-positron-photon interactions. We will discuss this contribution in detail to illustrate the method that we will use in the analysis of more complicated multi-loop diagrams.

At this point, we introduce some notational simplifications. We suppress the  $X$  dependence of all functions. All Green's functions used in our perturbative calculations correspond to free fields, and thus we suppress the index  $\nu'$  on these functions. Similarly, we suppress from now on the index  $\nu'$  which has been used to denote the free distribution function and the free spectral function. Finally, we define on-shell four-momenta

$$p = (E_p; \mathbf{p}); \quad (80)$$

with  $E_p = \sqrt{\mathbf{p}^2 + m^2}$ . We note that  $\sqrt{\mathbf{p}^2 + m^2}$  should be denoted  $E_p^0$ , but as above the index  $\nu'$  is suppressed.

The Keldysh selfenergies corresponding to the diagram from Fig. 2 are

$$\begin{aligned} \Sigma^+ (p) &= i \frac{g^2}{2} \int \frac{d^4 q}{(2\pi)^4} [ \Sigma^{\text{sym}}(q) \Sigma^+(q+p) + \Sigma^{\text{sym}}(q) \Sigma^+(q+p) ]; \\ \Sigma^- (p) &= i \frac{g^2}{2} \int \frac{d^4 q}{(2\pi)^4} [ \Sigma^{\text{sym}}(q) \Sigma^-(q+p) + \Sigma^+(q) \Sigma^{\text{sym}}(q+p) ]; \\ \Sigma^{\text{sym}} (p) &= i \frac{g^2}{2} \int \frac{d^4 q}{(2\pi)^4} [ \Sigma^{\text{sym}}(q) \Sigma^{\text{sym}}(q+p) + \Sigma^+(q) \Sigma^-(q+p) + \Sigma^-(q) \Sigma^+(q+p) ]; \end{aligned} \quad (81)$$

We substitute these selfenergies into the right hand side of the collision term (79) and express  $\Sigma^{\text{sym}}(p)$  through the distribution function according to Eq. (58). We also use Eqs. (45, 50) which give

$$\Sigma^+ (p) - \Sigma^- (p) = \text{sgn}(p_0) 2 \sqrt{\mathbf{p}^2 - m^2}; \quad (82)$$

and we observe that

$$\int \frac{d^4 q}{(2\pi)^4} \Sigma^+(q) \Sigma^+(q+p) = \int \frac{d^4 q}{(2\pi)^4} \Sigma^-(q) \Sigma^-(q+p) = 0; \quad (83)$$

due to the positions of poles. Thus, we obtain

$$\begin{aligned} (p_0) A(p) C_{1L}^{-3}(p) &= (p_0) \frac{g^2}{16} \int \frac{d^4 q}{(2\pi)^4} \sum_{\substack{f n_q; n_p; n_r; g=1 \\ X}} F_3(n_p; p; n_q; q; n_r; -r) \\ &\quad \sum_{Y} n \text{sgn}(p_0) 2 \sqrt{\mathbf{p}^2 - m^2} (n_0); \\ &= f(p; q; r; g) \end{aligned} \quad (84)$$

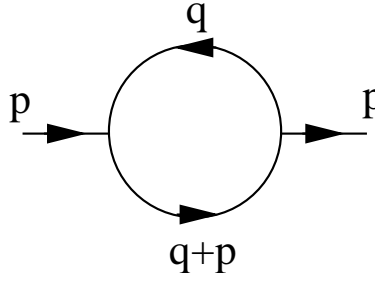
where  $r = q + p$  and  $n$  is a generic four-momentum variable which equals  $p, q$  or  $r$ , and  $n = \pm 1$ . The statistical factor  $F_N$  is defined as

$$\begin{aligned} F_N(n_1; p_1; n_2; p_2; \dots; n_N; p_N) &= (n_1; p_1) (n_2; p_2) \dots (n_N; p_N) \\ &\quad (n_1; p_1) (n_2; p_2) \dots (n_N; p_N) \end{aligned} \quad (85)$$

with

$$(n; p) = (1+n) 1 + f(p) + (1-n) f(-p); \quad (86)$$

We note that the asymmetry in the signs of  $(n_q; q)$  and  $(n_r; r)$  in the factor  $F_3(n_p; p; n_q; q; n_r; -r)$  occurs because the momenta  $q$  and  $r$  are defined to flow in opposite directions in Fig. 2.

FIG. 2: One-loop contribution to the  $\pi^3$  selfenergy.

To further simplify our result, we write the delta functions as

$$\delta(p_0 - (E^2 - m^2)) = \frac{1}{2E} \sum_{n=-1}^{\infty} \delta(p_0 - (E - nE)); \quad (87)$$

where  $E = \frac{p}{m^2 + p^2}$ , and get

$$(p_0) A(p) C_{1L}^{-3}(p) = (p_0) \frac{g^2}{16} \int \frac{d^4 q}{(2\pi)^4} \sum_{f n_p, m_q, m_r g=1}^{\infty} F_3(n_p; p; n_q; q; n_r; r) \sum_{f p; q; r g}^{\infty} \frac{1}{E} \delta(p_0 - nE) \quad (88)$$

We rewrite the expression (88) by introducing the delta function  $\delta^{(4)}(p + q - r)$  and an integral over  $r$ , which allows us to treat  $r$  as an independent variable. Performing the integrals over  $p_0$  and  $r_0$ , one obtains

$$(p_0) A(p) C_{1L}^{-3}(p) = (p_0) \frac{g^2}{64} \int \frac{d^3 q}{(2\pi)^3} \int \frac{d^3 r}{(2\pi)^3} \delta^{(3)}(p + q - r) \sum_{f p; q; r g}^{\infty} \frac{1}{E} \quad (89)$$

$$\sum_{f n_p, m_q, m_r g=1}^{\infty} (n_p E_p)^2 (n_p E_p + n_q E_q - n_r E_r) F_3(n_p; p; n_q; q; n_r; r)$$

We discuss below the physical interpretation of the positive energy piece of the collision term (89) which will be denoted with the index (+). We drop the theta function in Eq. (89) and take only the  $n_p = 1$  term in the sum. We also use the explicit form of the free spectral function (50) to make the replacement

$$(p_0) A(p) = \frac{1}{E_p} (p_0 - E_p): \quad (90)$$

In principle, we are left with four terms that come from the sum over  $n_q$  and  $n_r$  in Eq. (89). One of these terms corresponds to a delta function of the form  $\delta(E_p + E_q + E_r)$  which has no support. The remaining three terms correspond to the processes symbolically denoted as:  $p \rightarrow q + r$ ,  $p + q \rightarrow r$  and  $p + r \rightarrow q$ . The last two terms can be combined by making the variable transformation  $q \rightarrow r$  in the second term.

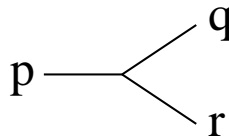
We consider first the contribution to the collision term (89) obtained from choosing  $n_q = 1$  and  $n_r = 1$ . Making the change of variables  $q \rightarrow r$ , we find

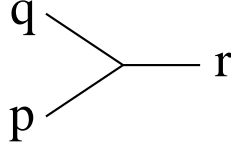
$$C_{1L}^{(+)-3}[p \rightarrow q + r] = \frac{g^2}{64} \int \frac{d^3 q}{(2\pi)^3 E_q} \int \frac{d^3 r}{(2\pi)^3 E_r} (2\pi)^4 \delta^{(4)}(p - q - r) E_3(1; p; 1; q; 1; r); \quad (91)$$

where the statistical factor equals

$$F_3(1; p; 1; q; 1; r) = \frac{1}{2} \frac{1 + f(p) f(q) f(r)}{1 + f(p) + f(q) + f(r)}: \quad (92)$$

This process is represented in Fig. 3.

FIG. 3:  $p \rightarrow q + r$  scattering process.

FIG. 4:  $p + q \rightarrow r$  scattering process.

Next, we look at the contributions to Eq. (89) obtained from choosing  $n_q = n_r = 1$  and  $n_q = n_r = -1$ . After changing variables and combining the two terms, we get

$$C_{1L}^{(+)}[p + q \rightarrow r] = \frac{g^2}{32} \int \frac{d^3 q}{(2\pi)^3 E_q} \int \frac{d^3 r}{(2\pi)^3 E_r} (2\pi)^4 \delta^{(4)}(p + q - r) F_3(1; q; 1; q; -1; -r); \quad (93)$$

with

$$F_3(1; p; 1; q; -1; -r) = \frac{1}{2} [1 + f(p) + 1 + f(q) + f(r) - f(p)f(q) + 1 + f(r)] : \quad (94)$$

This contribution is illustrated in Fig. 4.

The complete one-loop collision term equals

$$C_{1L}^{(+)}(p) = \int \frac{d^3 q}{(2\pi)^3 E_q} \int \frac{d^3 r}{(2\pi)^3 E_r} \mathcal{M}_{1L}^2 \int \frac{d^3 p}{(2\pi)^3 E_p} \delta^{(4)}(p + q - r) \frac{1}{2!} [1 + f(p) + f(q) + f(r) - f(p)f(q) + 1 + f(r)] \\ + \int \frac{d^3 q}{(2\pi)^3 E_q} \int \frac{d^3 r}{(2\pi)^3 E_r} \delta^{(4)}(p + q - r) [1 + f(p) + 1 + f(q) + f(r) - f(p)f(q) + 1 + f(r)] ; \quad (95)$$

where the scattering matrix element equals  $\mathcal{M}_{1L}^2 = g^2 = 4$ . The two terms proportional to  $f(p)$  correspond to ‘loss’ contributions and the terms proportional to  $(1 + f(p))$  correspond to ‘gain’ contributions. In the first term, which represents the process  $p \rightarrow q + r$ , there is the factor  $1/2!$  because of the integration over momenta of two identical particles in either final or initial scattering state.

We remind the reader that the contribution (95) to the collision term is identically zero because it is impossible to satisfy the delta function constraint. Physically, an on-shell particle of mass  $m$  cannot decay into two on-shell particles with the same masses. We have presented this calculation to illustrate the method that we will use in the analysis of more complicated multi-loop diagrams.

#### XIV. TWO-LOOP CONTRIBUTIONS

First we note that at any number of loops greater than one, there are two different kinds of diagrams that contribute to the self-energy. The first class contains diagrams that are built from diagrams of lower loop order by adding tadpole type insertions. An example is shown in Fig. 5. The contribution to the collision term from a diagram of this type has the same structure as the corresponding lower loop diagram with the addition of effective masses coming from the tadpole insertions. This type of diagram will not be discussed here. The second class of diagrams does not contain tadpoles. This is the type of diagram that we study in this paper. For the first few diagrams we give some of the details of the calculation but for the most part we focus on the final results.

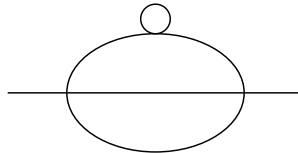


FIG. 5: Diagram with a tadpole insertion.



At the two-loop level, there are two contributions to the self-energy in  $\phi^3$  theory and one contribution in  $\phi^4$  theory (excluding diagrams with tadpoles).

#### A. $\phi^4$ theory

The two-loop contribution to self-energy is shown in Fig. 6. As in the case of the one-loop contribution in  $\phi^3$  theory, there is only one cut which is the central one. Calculating the retarded, advanced, and symmetric components of the self-energy, we obtain

$$\begin{aligned} \Sigma^+_{2L}(\mathbf{p}) &= \frac{g^2}{24} \int \frac{d^4 q}{(2\pi)^4} \int \frac{d^4 l}{(2\pi)^4} \int^h (q) \left[ \text{sym}(\mathbf{l}) \text{sym}(\mathbf{s}) + (\mathbf{l}) + (\mathbf{s}) \right. \\ &\quad \left. + \text{sym}(\mathbf{q}) (\mathbf{l}) \text{sym}(\mathbf{s}) + \text{sym}(\mathbf{l}) + (\mathbf{s}) \right] \frac{i}{E}; \end{aligned} \quad (96)$$

$$\begin{aligned} \Sigma(\mathbf{p}) &= \frac{g^2}{24} \int \frac{d^4 q}{(2\pi)^4} \int \frac{d^4 l}{(2\pi)^4} \int^h \left[ \text{sym}(\mathbf{s}) \text{sym}(\mathbf{q}) + (\mathbf{l}) + \text{sym}(\mathbf{l}) + (\mathbf{q}) \right. \\ &\quad \left. + (\mathbf{s}) \text{sym}(\mathbf{l}) \text{sym}(\mathbf{q}) + (\mathbf{l}) + (\mathbf{q}) \right] \frac{i}{E}; \end{aligned} \quad (97)$$

$$\begin{aligned} \Sigma^{\text{sym}}_{2L}(\mathbf{p}) &= \frac{g^2}{24} \int \frac{d^4 q}{(2\pi)^4} \int \frac{d^4 l}{(2\pi)^4} \int^h \left[ (\mathbf{l}) (\mathbf{s}) \text{sym}(\mathbf{q}) + \text{sym}(\mathbf{s}) + (\mathbf{q}) \right. \\ &\quad \left. + (\mathbf{l}) (\mathbf{q}) \text{sym}(\mathbf{s}) + \text{sym}(\mathbf{q}) + (\mathbf{s}) \right. \\ &\quad \left. + \text{sym}(\mathbf{l}) \text{sym}(\mathbf{q}) \text{sym}(\mathbf{s}) + (\mathbf{s}) + (\mathbf{q}) + (\mathbf{q}) + (\mathbf{s}) \right] \frac{i}{E}; \end{aligned} \quad (98)$$

where we have used  $\mathbf{s} = \mathbf{p} + \mathbf{q} + \mathbf{l}$ . We substitute these formulas into the collision term (79) and express the symmetric Green's function through the distribution function according to Eq. (58). As in the case of the one-loop diagram, we use Eqs. (82,83) to find

$$\begin{aligned} (\mathbf{p}_0) A(\mathbf{p}) C_{2L}(\mathbf{p}) &= (\mathbf{p}_0) \frac{g^2}{192} \int \frac{d^4 q}{(2\pi)^4} \int \frac{d^4 l}{(2\pi)^4} \\ &\quad \times \int_{f(\mathbf{n}_p; \mathbf{p}; \mathbf{n}_q; \mathbf{q}; \mathbf{n}_l; \mathbf{l}; \mathbf{n}_s; \mathbf{s})}^Y \frac{1}{E} \left( \mathbf{p}_0 - \mathbf{n}_E \right) : \\ &= f(\mathbf{p}; \mathbf{q}; \mathbf{l}; \mathbf{s}) \end{aligned} \quad (99)$$

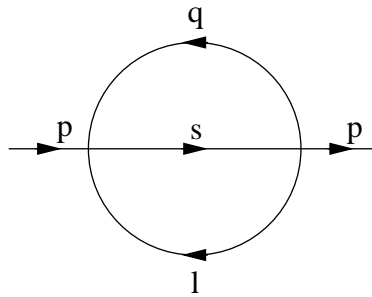


FIG. 6: Two-loop contribution to the  $\phi^4$  self-energy.

We rewrite the result (99) in a more symmetric way by introducing the delta function  $\delta^{(4)}(\mathbf{p} + \mathbf{q} + \mathbf{l} - \mathbf{s})$  and an integral over  $\mathbf{s}$ , which allows us to treat  $\mathbf{s}$  as an independent variable. As in the previous section, we use the free spectral function (90) and consider only positive energy contributions to the collision term. Performing the integrals over  $\mathbf{q}$ ,  $\mathbf{l}$ , and  $\mathbf{s}_0$ , we have

$$C_{2L}^{(+)}(\mathbf{p}) = \frac{g^2}{192} \int \frac{1}{(2\pi)^8} \int d^3 q \int d^3 l \int d^3 s \delta^{(3)}(\mathbf{p} + \mathbf{q} - \mathbf{l} - \mathbf{s}) \frac{1}{E_q E_l E_s} \quad (100)$$

X

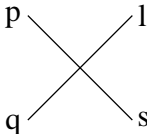
$$\text{fn}_{\text{p}}; \text{n}_1; \text{n}_s \text{g} = 1$$

$$\begin{aligned}
[1] \quad n_q &= n_l = n_s = 1; & l! & \quad l; & q! & \quad q; l! & \quad l; s! & \quad s; \\
[2] \quad n_q &= n_l = n_s = 1; & q! & \quad l; l! & \quad q; & q! & \quad l; l! & \quad q; s! & \quad s; \\
[3] \quad n_q &= n_l = n_s = 1; & q! & \quad s; l! & \quad l; s! & \quad q; q! & \quad s; l! & \quad l; s! & \quad q;
\end{aligned} \tag{101}$$

statistical factor defined by Eqs. (85,86), we finally find

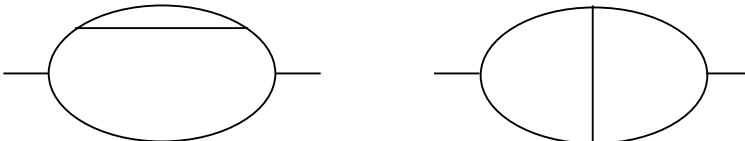
$$C_{2L}^{(+)}(p+q, s) = \frac{1}{2!} \frac{d^3 q}{(2\pi)^3 E_q} \frac{d^3 l}{(2\pi)^3 E_l} \frac{d^3 s}{(2\pi)^3 E_s} (2\pi)^4 \delta^{(4)}(q+p-l-s) M_{2L}^3 \frac{1}{4} \frac{1}{h} \frac{1+f(p)}{1+f(q)} \frac{1+f(l)}{f(l)} \frac{f(s)}{f(s)} \frac{f(p)}{f(q)} \frac{1+f(l)}{1+f(s)} \frac{1+f(s)}{1+f(s)} ; \quad (102)$$

where  $\mathcal{M}_{\text{PL}} = g^2 = 16$ . Eq. (102) gives the standard collision term corresponding to the binary process symbolically denoted as  $q + q \rightarrow l + s$  and illustrated in Fig. 7. The first (second) contribution is the usual gain (loss) term.

FIG. 7:  $p + q \rightarrow l + s$  scattering process.

### B. <sup>3</sup> theory

In  $^3$  theory, there are two graphs of different topologies that contribute at two-loop order as shown in Fig. 8.

FIG. 8: Contributions to the self-energy in  $^3$  theory.

The results for the self-energies are as follows

$$\begin{aligned}
+ \quad & \frac{g^4}{8} \frac{d^4 q}{(2)^4} \frac{d^4 k}{(2)^4} \left\{ \begin{aligned} & (q) \quad (r) \quad \text{sym} \quad (r) \quad (l) \quad \text{sym} \quad (k) + \quad \text{sym} \quad (l) \quad + \quad (k) \\ & + \quad (q) \quad (r) \quad + \quad (r) \quad \text{sym} \quad (k) \quad \text{sym} \quad (l) + \quad (l) \quad + \quad (k) + \quad (k) \quad + \quad (l) \\ & + \quad (q) \quad \text{sym} \quad (r) \quad + \quad (r) \quad (k) \quad \text{sym} \quad (l) + \quad \text{sym} \quad (k) \quad + \quad (l) \\ & + \quad \text{sym} \quad (q) \quad + \quad (r)^2 \quad (k) \quad \text{sym} \quad (l) + \quad \text{sym} \quad (k) \quad + \quad (l) \quad ; \end{aligned} \right. \quad (103)
\end{aligned}$$

$$\begin{aligned}
(p) = & \frac{g^4}{8} \frac{d^4 q}{(2)^4} \frac{d^4 k}{(2)^4} \left[ (r)^2 \text{sym}(q) (l) \text{sym}(k) + \text{sym}(l) + (k) \right. \\
& + (r) (r) \text{sym}(r) (l) \text{sym}(k) + \text{sym}(l) + (k) \\
& + (r) + (p) + (r) \text{sym}(k) \text{sym}(l) + (l) + (k) + (k) + (l) \\
& \left. + \text{sym}(r) + (p) + (r) (k) \text{sym}(l) + \text{sym}(k) + (l) \right] ;
\end{aligned} \tag{104}$$

$$\begin{aligned}
\text{sym}(p) = & \frac{g^4}{8} \frac{d^4 q}{(2)^4} \frac{d^4 k}{(2)^4} \left[ (r) \text{sym}(r) \text{sym}(q) (l) \text{sym}(k) + \text{sym}(l) + (k) \right. \\
& + (r) \text{sym}(r) \text{sym}(q) (k) \text{sym}(l) + \text{sym}(k) + (l) \\
& + (r)^2 + (q) (l) \text{sym}(k) + \text{sym}(l) + (k) \\
& + (r)^2 (q) (k) \text{sym}(l) + \text{sym}(k) + (l) \\
& \left. + (r) + (r) \text{sym}(q) \text{sym}(k) \text{sym}(l) + (l) + (k) + (k) + (l) \right] ;
\end{aligned} \tag{105}$$

We substitute these expressions into the collision term (79) and divide the results into contributions of three different types, which correspond to contributions to the three cuts shown in Fig. 9.

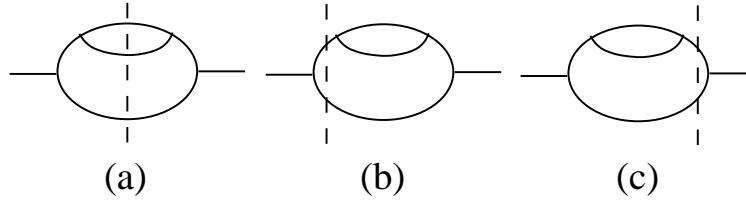


FIG. 9: Cuts of the first diagram in Fig. 8.

These cuts are referred to as the 'central', 'left' and 'right' cuts, respectively. Terms that contain a factor  $+(r) (r)$  correspond to the central cut. The terms with  $+(r)$  but without  $(r)$  are associated with the right cut, and terms that contain  $(r)$  but not  $+(r)$  correspond to the left cut. The results read:

$$\begin{aligned}
(p_0) A(p) C(p)_{\text{central}} = & (p_0) \frac{g^4}{64} \frac{d^4 q}{(2)^4} \frac{d^4 l}{(2)^4} + (r) (r) \\
& \times \int_{n_p, m_q, m_l, m_s = 1}^Y F_4(n_p; p; n_q; q; n_l; l; n_s; s) \frac{1}{E} (0 \text{ } n \text{ } E); \\
& = f(p; q; l; s)
\end{aligned} \tag{106}$$

$$\begin{aligned}
(p_0) A(p) C(p)_{\text{right}} = & (p_0) \frac{g^2}{32} \frac{d^4 q}{(2)^4} + (r) + (r) \\
& \times \int_{n_p, m_q, m_r = 1}^Y F_3(n_p; p; n_q; q; n_r; r) \frac{1}{E} (0 \text{ } n \text{ } E); \\
& = f(p; q; r)
\end{aligned} \tag{107}$$

$$\begin{aligned}
(p_0) A(p) C(p)_{\text{left}} = & (p_0) \frac{g^2}{32} \frac{d^4 q}{(2)^4} (r) (r) \\
& \times \int_{n_p, m_q, m_r = 1}^Y F_3(n_p; p; n_q; q; n_r; r) \frac{1}{E} (0 \text{ } n \text{ } E); \\
& = f(p; q; r)
\end{aligned} \tag{108}$$

In Eqs. (107) and (108) the factors  $+(r)$  and  $(r)$  refer to one-loop selfenergies of the form shown in Fig. 2. Thus, we find that the non-central cuts give contributions that can be understood as corrections to the one-loop result as shown in Fig. 10.

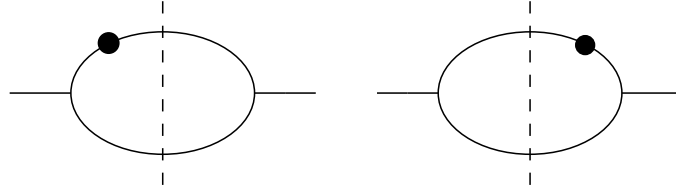


FIG .10: Non-central cut for the first diagram in Fig. 8.

Non-central cuts can always be treated in this manner i.e. every non-central cut provides a higher order correction to the central cut of some other diagram. As explained in the Introduction, we are only interested in the dominant contributions to any given physical process, and consequently we consider only central cuts from now on. We calculate contributions to the collision term at leading order in  $g$  for each physical process from the relevant sum of centrally cut self-energy diagrams at the same order of  $g$ . The collision term contains some phase space integrals, the statistical factor  $F_N$  (Eq. (85)), and the square of a matrix element which is constructed from uncut propagators. At higher orders in  $g$ , there are many self-energy diagrams that have to be included, some of which have more than one central cut. It is a non-trivial technical problem to combine all of these terms into a result which can be written as the square of a matrix element. This structure is obtained by an appropriate choice of momentum labels for the internal lines of the self-energy diagrams. We proceed as follows:

- 1) the same set of momentum variables is always assigned to the cut propagators (equivalently, each central cut has the same  $F$  factor);
- 2) all possible permutations of momentum variables for the uncut lines are considered;
- 3) for each diagram, all permutations are summed and the sum is normalized with the appropriate weight.

Using this strategy, we calculate the nine diagrams shown in Figs. 11 and 12 where we have made the following definitions for momentum variables:

$$r = p + q; \quad t = q + l; \quad h = p + l; \quad s = r + l: \quad (109)$$

We note that the second topology in Fig. 8 appears twice as often as the first topology (six times as compared with three) because of the fact that we take only one of two possible diagonal cuts for these diagrams.

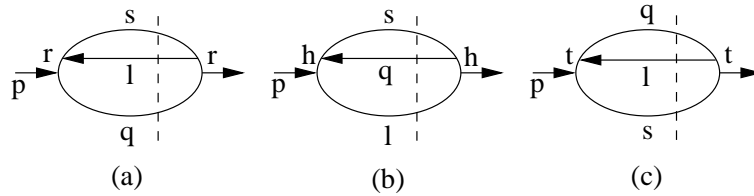


FIG .11: Three permutations of the centrally cut first diagram in Fig. 8.



The matrix element squared is given by

$$M_{2L}^2 = \frac{g^4}{16} \left( \frac{1}{S} + \frac{1}{T} + \frac{1}{U} \right); \quad (114)$$

where  $S$ ,  $T$ , and  $U$  are the Mandelstam variables defined as

$$S = (q + p)^2; \quad T = (l + p)^2; \quad U = (q + l)^2; \quad (115)$$

We have used here capital letters to avoid confusion with momentum variables. This matrix element is illustrated in Fig. 13.

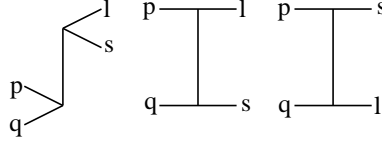


FIG. 13: Scattering diagrams that contribute to the process  $p + q \rightarrow l + s$  in  $\phi^4$  theory.

## XV. THREE-LOOP CONTRIBUTIONS

### A. $\phi^4$ theory

In  $\phi^4$  theory, the only three-loop diagram that does not involve tadpoles is shown in Fig. 14a. This diagram does not have a central cut. The non-central cut presented in Fig. 14a produces a correction to the two-loop sunset graph, as shown in Fig. 14b, and will not be discussed.

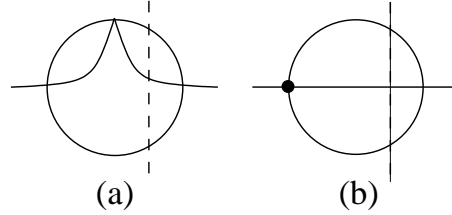


FIG. 14: Three-loop contribution to the  $\phi^4$  self-energy (a); and an effective two-loop contribution containing a corrected vertex function (b).

### B. $\phi^3$ theory

There are diagrams of eight different topologies which contribute to the  $\phi^3$  self-energy at the three-loop level. They are shown in Fig. 15.

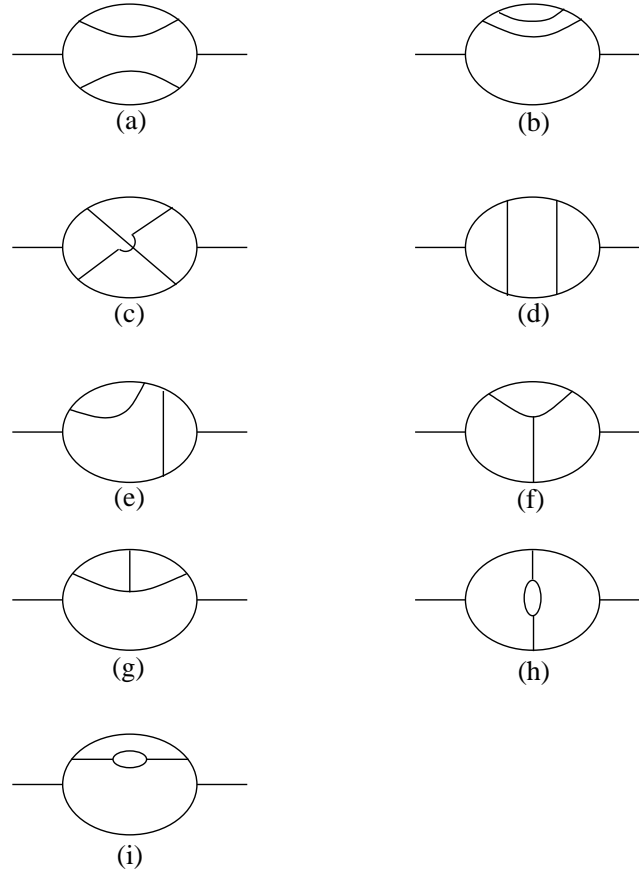


FIG. 15: Three-loop contributions to the  $\pi^3$  self-energy.

We follow the same strategy as in the previous section and consider only the central cuts of the diagrams in Fig. 15. The internal lines are labeled in all possible ways that produce the same statistical factor. In addition to the definition (109), we define the following momentum variables:

$$\begin{aligned} y &= q+k; & m &= k+l; & j &= k+p; & z &= p+q+k; \\ w &= q+k+l; & v &= p+k+l; & u &= p+q+k+l; \end{aligned} \quad (116)$$

In analogy to Eq. (110), we define the operation

$$\begin{aligned} \pi_{3L}^{(3)} &\stackrel{\text{def}}{=} (p_0) \frac{g^6}{64} \int \frac{d^4 k}{(2\pi)^4} \int \frac{d^4 l}{(2\pi)^4} \int \frac{d^4 q}{(2\pi)^4} \\ &\quad \times \int_{f(n_p; n_q; n_l; n_k; n_u)g=1}^X F_5(n_p; p; n_q; q; n_l; l; n_k; k; n_u; u) \int^Y \frac{1}{E} (0 \leq n \leq E) \\ &\quad = f(p; q; l; k; u)g \end{aligned} \quad (117)$$

Combining the results for the diagrams in Figs. 15a–15h, we obtain

$$\begin{aligned} (p_0) A(p) C_{3L}^{(3)}(p) &= \frac{1}{24} \left[ (t) + (s) + (y) + (z) + (m) + (v) \right. \\ &\quad + (n) + (r) + (x) + (z) + (x) + (s) + (h) + (v) \\ &\quad + (y) + (h) + (h) + (s) + (t) + (j) + (v) + (j) \\ &\quad \left. + (z) + (j) + (m) + (w) + (t) + (w) + (y) + (w) \right] \pi_{3L}^{(3)} : \end{aligned} \quad (118)$$

We can rewrite the result (118) by introducing the delta function  $\delta^{(4)}(p + q + k + l - u)$  and an integral over  $u$ . As we have done previously, we use Eq. (90) and consider only positive energy contributions to the collision term. The sum over  $n_q, n_l, n_k$ , and  $n_u$  produces 16 terms. Of these 16 terms, 10 are kinematically allowed. Four of these processes can be combined by relabeling momentum variables to produce the process symbolically denoted as  $p + q \rightarrow l + k + u$ . The remaining six can be combined to produce the process of the form  $p + q \rightarrow l + k + u$ .

#### The process $p + q \rightarrow l + k + u$

We list the four possible choices of the  $n$ 's and the variable transformations that allow us to combine terms and obtain the matrix element corresponding to the process  $p + q \rightarrow l + k + u$ :

$$\begin{aligned}
 [1] \quad n_q = n_l = n_k = n_u = 1; \quad l! &= l; k! = k; \quad q! = q; l! = l; \\
 & \quad k! = k; u! = u; \\
 [2] \quad n_q = n_l = n_k = n_u = 1; \quad q! &= k; k! = q; \quad q! = k; l! = l; \\
 & \quad l! = l; \quad k! = q; u! = u; \\
 [3] \quad n_q = n_l = n_k = n_u = 1; \quad q! &= l; l! = q; \quad q! = l; l! = q; \\
 & \quad k! = k; \quad k! = k; u! = u; \\
 [4] \quad n_q = n_l = n_k = n_u = 1; \quad q! &= u; l! = l; \quad q! = u; k! = k; \\
 & \quad k! = k; u! = u; \quad q! = l; u! = u;
 \end{aligned} \tag{119}$$

The delta functions and statistical factor have the same form for each of these four terms. A straightforward but very tedious calculation verifies that the same matrix element is produced in each case. The collision term representing the process  $p + q \rightarrow l + k + u$  equals

$$\begin{aligned}
 C_{3L}^{(+)}[p + q \rightarrow l + k + u] &= \frac{1}{3!} \frac{d^3 q}{(2\pi)^3 E_q} \frac{d^3 l}{(2\pi)^3 E_l} \frac{d^3 k}{(2\pi)^3 E_k} \frac{d^3 u}{(2\pi)^3 E_u} \\
 & \quad (2\pi)^4 \delta^{(4)}(p + q - l - k - u) \mathcal{M}_{3L}^2[p + q \rightarrow l + k + u] \\
 & \quad \frac{1}{1 + f(p)} \frac{1}{1 + f(q)} \frac{1}{f(l)} \frac{1}{f(k)} \frac{1}{f(u)} \frac{1}{f(p)} \frac{1}{f(q)} \frac{1}{1 + f(l)} \frac{1}{1 + f(k)} \frac{1}{1 + f(u)} ;
 \end{aligned} \tag{120}$$

where the matrix element squared of the diagrams shown in Fig. 16 is

$$\begin{aligned}
 \mathcal{M}_{3L}^2[p + q \rightarrow l + k + u] &= \frac{g^6}{2^5} \left( (p + q) \cdot (k + l) + (k + u) \cdot (l + u) + (l + u) \cdot (p + q) \right. \\
 & \quad + (p \cdot l) + (q \cdot k) + (q \cdot u) + (k \cdot u) \\
 & \quad + (p \cdot k) + (q \cdot l) + (q \cdot u) + (l \cdot u) \\
 & \quad + (p \cdot u) + (q \cdot l) + (q \cdot k) + (l \cdot k) \\
 & \quad \left. + (q \cdot l) \cdot (k + u) + (q \cdot k) \cdot (l + u) + (q \cdot u) \cdot (l + k) \right)^2 ;
 \end{aligned} \tag{121}$$



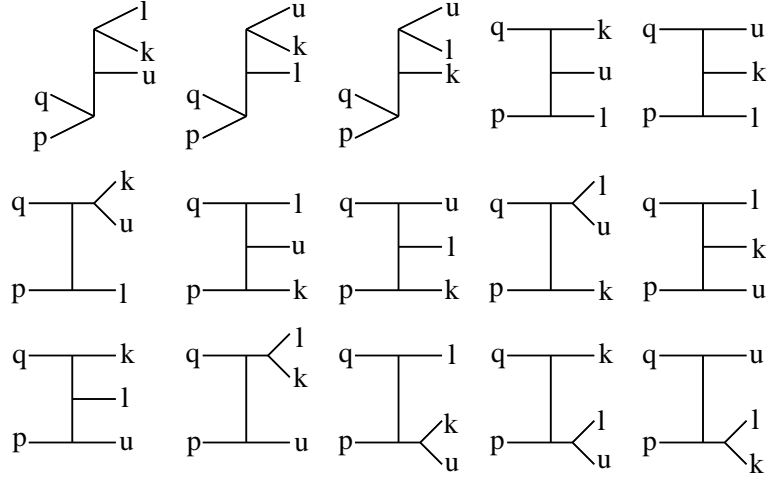


FIG. 16: Scattering diagrams that contribute to the process  $p + q \rightarrow l + k + u$  in the order they appear in Eq. (121).

### The process $q + p \rightarrow l + k + u$

We list the six possible choices of the  $n$ 's and the variable transformations that allow us to combine terms and obtain the matrix element corresponding to the process  $p + q \rightarrow l + k + u$ :

$$\begin{aligned}
 [1] \quad & n_q = n_l = n_k = n_u = 1; \quad k \rightarrow k; \quad l \rightarrow l; \\
 [2] \quad & n_q = n_l = n_k = n_u = 1; \quad l \rightarrow k; k \rightarrow l; \quad l \rightarrow k; k \rightarrow l; \\
 [3] \quad & n_q = n_l = n_k = n_u = 1; \quad p \rightarrow k; k \rightarrow p; \quad p \rightarrow k; k \rightarrow p; \\
 [4] \quad & n_q = n_l = n_k = n_u = 1; \quad l \rightarrow u; k \rightarrow k; \quad l \rightarrow u; k \rightarrow k; \\
 [5] \quad & n_q = n_l = n_k = n_u = 1; \quad p \rightarrow u; k \rightarrow l; \quad p \rightarrow u; k \rightarrow l; \\
 [6] \quad & n_q = n_l = n_k = n_u = 1; \quad p \rightarrow u; l \rightarrow k; \quad p \rightarrow u; l \rightarrow k;
 \end{aligned} \tag{122}$$

The delta functions and statistical factors have the same form for each of these six terms. Similarly, one can verify that the matrix element is the same in each case. The contribution to the collision term from  $p + q \rightarrow l + k + u$  processes is

$$\begin{aligned}
 C_{3L}^{(+)}[p + q \rightarrow l + k + u] = & \frac{1}{2!2!} \int \frac{d^3q}{(2\pi)^3 E_q} \int \frac{d^3l}{(2\pi)^3 E_l} \int \frac{d^3k}{(2\pi)^3 E_k} \int \frac{d^3u}{(2\pi)^3 E_u} \\
 & (2\pi)^4 \delta^4(p + q - l - k - u) \mathcal{M}_{3L}^2[p + q \rightarrow l + k + u] \\
 & \times [1 + f(p)][1 + f(q)][1 + f(l)]f(k)f(u) - f(p)f(q)f(l)[1 + f(k)][1 + f(u)];
 \end{aligned} \tag{123}$$

where the matrix element squared of the diagrams shown in Fig. 17 equals

$$\begin{aligned}
 \mathcal{M}_{3L}^2[p + q \rightarrow l + k + u] = & \frac{g^6}{2^5} \left[ (p + q)(k + l) + (k + u)(l + p) + (l + u)(p + q) \right. \\
 & + (p + l)(q + k) + (q + l)(k + u) + (k + l)(p + u) \\
 & \left. + (p + k)(q + l) + (q + k)(l + u) + (l + u)(p + k) \right]
 \end{aligned} \tag{124}$$

$$\begin{aligned}
& + (\mathfrak{p} \quad \mathfrak{x}) + (\mathfrak{q} + \mathfrak{l}) + (\mathfrak{q} \quad \mathfrak{k}) + (\mathfrak{l} + \mathfrak{k}) \\
& + (\mathfrak{q} + \mathfrak{l}) (\mathfrak{k} + \mathfrak{x}) + (\mathfrak{q} \quad \mathfrak{k}) (\mathfrak{l} + \mathfrak{x}) + (\mathfrak{q} \quad \mathfrak{x}) (\mathfrak{l} + \mathfrak{k})^2 :
\end{aligned}$$

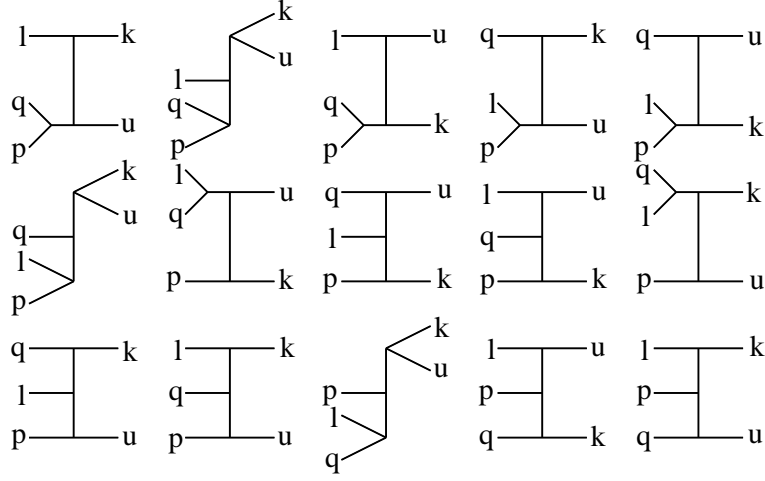


FIG .17: Scattering diagrams that contribute to the process  $p + q + l \rightarrow k + u$  in the order they appear in Eq. (124).

The collision term for  $\mathcal{E}^3$  theory at the three-loop level, which represents the  $2 \times 3$  processes, is given by the sum of the contributions (120,123). Such a form of the collision term was postulated in [9, 10] to reproduce the Kubo formula result of the viscosity coefficients within a linearized kinetic theory.

#### XVI. FOUR-LOOP CONTRIBUTIONS

At the four-loop level, we consider only  $\mathcal{E}^4$  theory. The relevant diagrams are the double sunset and two crossed versions of the double sunset, as shown in Fig 18. All other contributions contain tadpoles and will not be discussed, as has been previously explained.

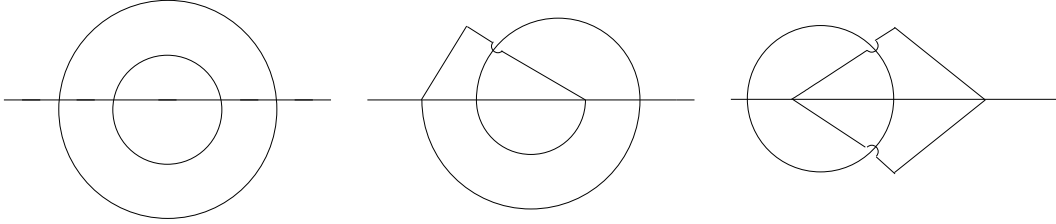


FIG .18: Four-loop contributions to the  $\mathcal{E}^4$  self-energy.

We follow the strategy formulated in Sec. XIV B and label internal lines of the diagrams in all possible ways that produce the same statistical factor. As previously, we define the operation

$$\begin{aligned}
\mathcal{E}^{4L} &\stackrel{\text{def}}{=} (\mathfrak{p}_0) \frac{g^4}{1536} \frac{d^4 \mathfrak{q}}{(2)^4} \frac{d^4 \mathfrak{l}}{(2)^4} \frac{d^4 \mathfrak{m}}{(2)^4} \frac{d^4 \mathfrak{k}}{(2)^4} \\
&\quad \times \int \mathfrak{p} \mathfrak{q} \mathfrak{l} \mathfrak{m} \mathfrak{k} \mathfrak{x} g = 1 \\
&\quad \times \frac{1}{E} (\mathfrak{p}_0 \quad \mathfrak{n} \quad \mathfrak{E}) \\
&= f(\mathfrak{p}; \mathfrak{q}; \mathfrak{l}; \mathfrak{m}; \mathfrak{k}; \mathfrak{x}) g
\end{aligned} \tag{125}$$

where we have used the definitions (109) and (116), and additionally, we have introduced  $x = q + p + k + l + m$ . After summing up all central cuts of the diagrams shown in Fig 18, we get the four-loop collision term

$$\begin{aligned}
 (p_0) A(q) C_{4L}^{(+)}(p) = & \frac{1}{10} \left[ (p+q+k) + (p+q+l) + (p+q+m) \right. \\
 & + (p+k+l) + (p+k+m) + (p+l+m) \\
 & \left. + (k+l+m) + (q+k+l) + (q+l+m) + (q+k+m)^2 \right]_{4L}^{(+)} :
 \end{aligned} \quad (126)$$

We rewrite this result by introducing the delta function  $\delta^{(4)}(q + p + k + l + m - x)$  and an integral over  $x$ . As we have done previously, we will use Eq. (90) and consider only positive energy contributions to the collision term. The sum over the remaining  $n$ 's contains 32 terms. Five of these terms can be combined to give the process  $p + q \rightarrow k + l + m + x$ , ten give the process  $p + q + l + m \rightarrow k + x$ , and ten give the process  $p + q + l \rightarrow m + k + x$ . The remaining seven terms are kinematically forbidden. Below, we give the collision terms representing these processes.

The process  $p + q \rightarrow k + l + m + x$

$$\begin{aligned}
 C_{4L}^{(+)}[p + q \rightarrow l + k + m + x] = & \frac{1}{4!} \int \frac{d^3 q}{(2)^3 E_q} \int \frac{d^3 l}{(2)^3 E_l} \int \frac{d^3 k}{(2)^3 E_k} \int \frac{d^3 m}{(2)^3 E_m} \int \frac{d^3 x}{(2)^3 E_x} \\
 & (2)^4 \delta^{(4)}(p + q - l - k - m - x) M_{4L}^{2i} [p + q \rightarrow l + k + m + x] \\
 & h \\
 & 1 + f(p) \quad 1 + f(q) \quad f(l) f(k) f(m) f(x) \\
 & f(p) f(q) \quad 1 + f(l) \quad 1 + f(k) \quad 1 + f(m) \quad 1 + f(x) \quad ;
 \end{aligned} \quad (127)$$

where the matrix element squared of the diagrams shown in Fig. 19 equals

$$\begin{aligned}
 M_{4L}^2 [p + q \rightarrow l + k + m + x] = & \frac{g^4}{2^6} \left[ (k + l + m) + (q - k - l) + (q - k - m) \right. \\
 & + (q - l - m) + (p - k - l) + (p - k - m) \\
 & \left. + (p - l - m) + (p + q - k) + (p + q - l) + (p + q - m)^2 \right] :
 \end{aligned} \quad (128)$$

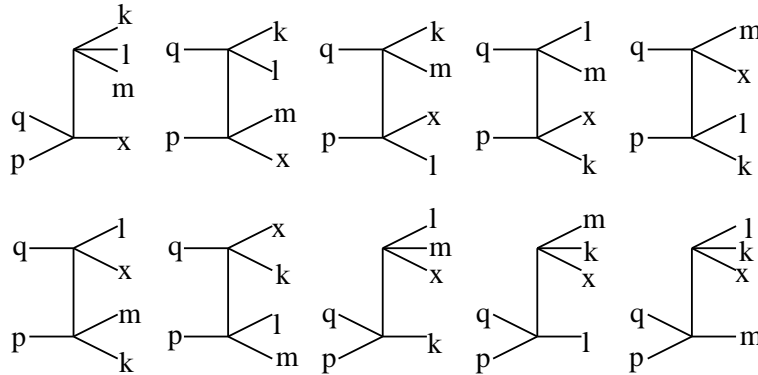


FIG. 19: Scattering diagrams that contribute to the process  $p + q \rightarrow k + l + m + x$  in the order they appear in Eq. (128).

The process  $p + q + l + m \rightarrow k + x$

$$\begin{aligned}
C_{4L}^{(+)}[p+q+l+m \rightarrow k+x] &= \frac{1}{3!2!} \frac{d^3 q}{(2)^3 E_q} \frac{d^3 l}{(2)^3 E_l} \frac{d^3 m}{(2)^3 E_m} \frac{d^3 k}{(2)^3 E_k} \frac{d^3 x}{(2)^3 E_x} \quad (129) \\
&= (2)^4 (4) (p+q+l+m \rightarrow k+x) \mathcal{M}_{4L}^2[p+q+l+m \rightarrow k+x] \\
&\quad \times \frac{1}{h} \frac{1+f(p)}{1+f(q)} \frac{1+f(l)}{1+f(m)} \frac{1+f(k)}{1+f(x)} \\
&\quad \times \frac{1}{f(p)f(q)f(l)f(m)} \frac{1+f(k)}{1+f(x)} ;
\end{aligned}$$

where the matrix element squared of the diagrams shown in Fig. 20 equals

$$\begin{aligned}
\mathcal{M}_{4L}^2[p+q+l+m \rightarrow k+x] &= \frac{g^4}{2^6} + (l+m \rightarrow k) + (q \rightarrow k+l) + (q \rightarrow k+m) \\
&+ (q+l+m) + (p \rightarrow k+l) + (p \rightarrow k+m) \\
&+ (p+l+m) + (p+q \rightarrow k) + (p+q+l) + (p+q+m)^2 : \quad (130)
\end{aligned}$$

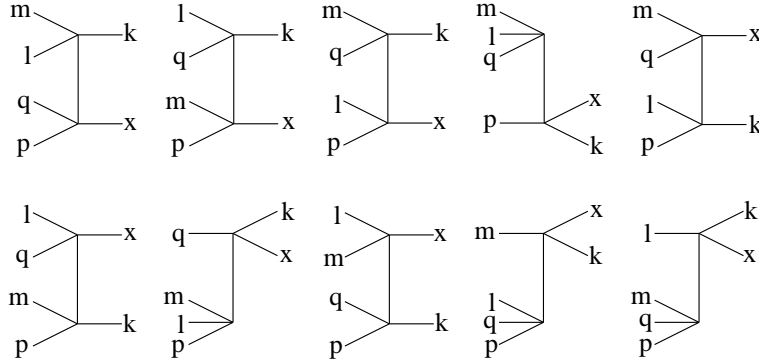


FIG. 20: Scattering diagrams that contribute to the process  $p+q+l+m \rightarrow k+x$  in the order they appear in Eq. (130).

#### The process $p+q+l \rightarrow m+k+x$

$$\begin{aligned}
C_{4L}^{(+)}[p+q+l \rightarrow m+k+x] &= \frac{1}{2!3!} \frac{d^3 q}{(2)^3 E_q} \frac{d^3 l}{(2)^3 E_l} \frac{d^3 m}{(2)^3 E_m} \frac{d^3 k}{(2)^3 E_k} \frac{d^3 x}{(2)^3 E_x} \quad (131) \\
&= (2)^4 (4) (p+q+l \rightarrow m+k+x) \mathcal{M}_{4L}^2[p+q+l \rightarrow m+k+x] \\
&\quad \times \frac{1}{h} \frac{1+f(p)}{1+f(q)} \frac{1+f(l)}{f(m)} \frac{f(k)}{1+f(x)} \\
&\quad \times \frac{1}{f(p)f(q)f(l)} \frac{1+f(m)}{1+f(k)} \frac{1+f(x)}{1+f(x)} ;
\end{aligned}$$

where the matrix element squared of the diagrams shown in Fig. 21 equals

$$\begin{aligned}
\mathcal{M}_{4L}^2[p+q+l \rightarrow m+k+x] &= \frac{g^4}{2^6} + (l \rightarrow k+m) + (q \rightarrow k+l) + (q \rightarrow k+m) \\
&+ (q+l \rightarrow m) + (p \rightarrow k+l) + (p \rightarrow k+m) \\
&+ (p+l \rightarrow m) + (p+q \rightarrow k) + (p+q+l) + (p+q+m)^2 : \quad (132)
\end{aligned}$$

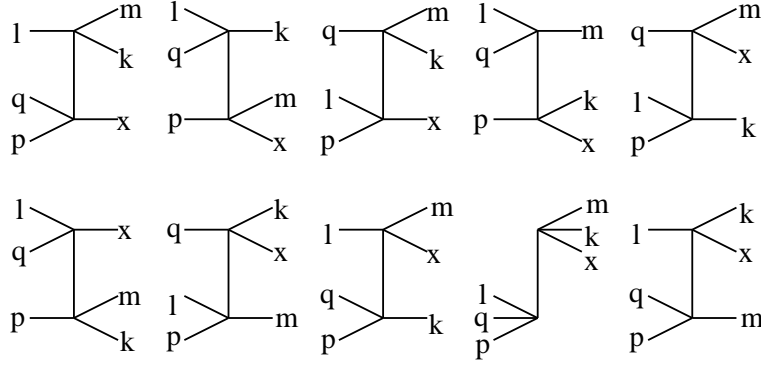


FIG. 21: Scattering diagrams that contribute to the process  $p + q + l \rightarrow m + k + x$  in the order they appear in Eq. (132).

The collision term of the  $\epsilon^4$  theory at four-loop level, which represents the  $2\epsilon^4$  and  $3\epsilon^3$  processes, is given by the sum of the contributions (127,129,131). As in the case of  $\epsilon^3$  interaction, a form of the collision term beyond binary approximation was postulated in [9, 10] to reproduce the Kubo formula result of the viscosity coefficients within a linearized kinetic theory. While the contributions representing the  $2\epsilon^4$  processes coincide, the term corresponding to the  $3\epsilon^3$  interactions is absent in the effective transport equation [9, 10], as it is supposed to give negligible contribution to the viscosity [41]. As already mentioned, the scattering  $3\epsilon^3$  was discussed in [8].

In performing the perturbative calculations of the collision terms in Secs. XIII-XV I, we have used non-interacting Green's functions. However, the transport equation is of interest precisely because its solution is the full interacting distribution function. The terms on the left hand side of the transport equation clearly depend on this interacting distribution function. On the right hand side, we use the perturbatively calculated collision term and replace the non-interacting distribution function by the interacting one. We drop gradient terms in the expansion of the interacting distribution function about the non-interacting distribution, when these gradient terms appear within the collision term. The justification for this procedure is as follows: we consider the gradient and coupling constant approximations as independent, and choose to investigate higher order terms in the coupling constant approximation, while working at lowest order in the gradient approximation. The contributions we have calculated correspond physically to multiparticle production processes involving zero width quasi-particles. We remind the reader that finite width quasi-particles will give rise to contributions to the collision term that are kinematically forbidden for zero-width quasi-particles. For  $\epsilon^4$  theory an example is a  $1\epsilon^3$  process. In this paper we assume infinitely narrow quasi-particles (Eq. (29)), and in this limit the effects of these processes will be negligible.

## XVII. SUMMARY AND OUTLOOK

Kinetic equations usually take into account the interaction of particles with a mean field, and inter-particle pair collisions. However, when the system of interest is very dense, multiparticle interactions are expected to play a significant role in the system's dynamics. In addition, if a characteristic particle's kinetic energy is comparable to the particle's mass, particle production processes become important. Both multiparticle interactions and production processes occur in systems of relativistic quantum fields, such a quark-gluon plasma, when the energy density is sufficiently high.

In this study, we have given the first systematic derivation of the transport equation of relativistic quantum fields which takes into account multiparticle and production process. Using the Schwinger-Keldysh approach, we have discussed scalar fields with cubic and quartic interactions. Mean-field phenomena are controlled by the one-loop tadpole contributions to the self-energy, and binary collisions correspond to the two-loop graphs. Multiparticle process occur at the three-loop level in  $\epsilon^3$  theory and at the four-loop level in  $\epsilon^4$  theory. Analysis of three- and four-loop diagrams is a technically very complex problem which requires special computational techniques. We have used the Keldysh representation because it provides a clean separation between propagators that correspond to real and virtual particles. In addition, we have made use of the cut structure of the collision term. Our calculations have been performed with the help of a program that uses MATHEMATICA symbolic manipulation software.

Throughout this paper, we have assumed that quasi-particles are of zero-width and that their four-momenta are on the mass-shell. This assumption is crucial since some processes which occur at one- and two-loop level, like  $1\epsilon^2$  and  $1\epsilon^3$  processes, are kinematically forbidden for on-mass-shell particles. We have derived the explicit form of the contributions to the collision term of the transport equation corresponding to the processes:  $2\epsilon^3$  for the  $\epsilon^3$  model,

and  $2 \leq 4$  and  $3 \leq 3$  for the  $^4$  model.

In this paragraph we clearly state the domain of applicability of our final results. Our derivation relies on several assumptions and approximations which are discussed in Sec. V. First of all, the system has to be homogeneous at a scale which is smaller than or comparable to the characteristic inverse momentum and the inverse effective mass, as required by the conditions (26,27). The system has to be weakly interacting so that the loop expansion is a legitimate approximation. This requires smallness of the coupling constants. Since we consider quasiparticles which are on the mass shell, the conditions (27) and (29) have to be fulfilled. The latter is easily satisfied if the bare mass is much larger than the medium correction to the mass. A system of weakly interacting massive scalar fields which is close to equilibrium satisfies all of these conditions.

In the future we plan to study further the multi-particle collision terms derived here. Although the integrals seem to be regular for massive particles, they require very careful analysis, as the transport theory of dense gases or liquids is known to suffer serious problems at the level of multi-particle interactions, see e.g. [42]. The integral representing the process  $3 \rightarrow 3$  is of particular concern here as one particle can experience zero momentum transfer producing a singularity of the respective propagator.

We intend to extend the work of Refs. [9, 10] on the role of multi-particle processes in transport phenomena. However, we are going to start with the transport equations, which are derived here, and not with the Kubo formulas. We also plan to study how the system reaches chemical equilibrium due to particle production processes. The first step in this direction is to compute the interaction rate

$$[\Gamma]_{\text{def}} = \frac{1}{n} \sum_p \frac{d^3 p}{(2\pi)^3 E_p} C^{(+)} [p + p_1 + p_2 + \dots, n-1; q_1 + q_2 + \dots, m+1; q] \quad (133)$$

where  $C^{(+)} [ \dots ]$  is the gain contribution to the collision term corresponding to the process  $p + p_2 + \dots, n-1; q_1 + q_2 + \dots, m+1$ . Relative rates of the form  $[\Gamma]_{\text{def}} [2 \rightarrow 3] = [\Gamma]_{\text{def}} [2 \rightarrow 2]$  or  $[\Gamma]_{\text{def}} [3 \rightarrow 3] = [\Gamma]_{\text{def}} [2 \rightarrow 2]$  will give a measure of the importance of multi-particle processes.

#### Acknowledgments

This project was initiated at the program 'QCD and Gauge Theory Dynamics in the RHIC Era' organized by Kavli Institute for Theoretical Physics in Santa Barbara in April-June 2002. We are thus very grateful to the National Science Foundation for support under Grant No. PHY 99-07949.

- 
- [1] J.P. Hansen and I.R. McDonald, *Theory of Simple Liquids* (Academic Press, London, 1976).
  - [2] L. Xiong and E.V. Shuryak, *Phys. Rev. C* 49, 2203 (1994) [[arXiv:hep-ph/9309333](#)].
  - [3] K. Geiger and B. Müller, *Nucl. Phys. B* 369, 600 (1992).
  - [4] D.K. Srivastava and K. Geiger, *Nucl. Phys. A* 647, 136 (1999) [[arXiv:nucl-th/9806050](#)].
  - [5] R. Baier, A.H. Mueller, D. Schi and D.T. Son, *Phys. Lett. B* 502, 51 (2001) [[arXiv:hep-ph/0009237](#)].
  - [6] P. Arnold, G.D. Moore and L.G. Ya, *JHEP* 0301, 030 (2003) [[arXiv:hep-ph/0209353](#)].
  - [7] S.M.H. Wong, [arXiv:hep-ph/0404222](#).
  - [8] X.M. Xu, Y. Sun, A.Q. Chen and L. Zheng, *Nucl. Phys. A* 744, 347 (2004).
  - [9] S. Jeon, *Phys. Rev. D* 52, 3591 (1995) [[arXiv:hep-ph/9409250](#)].
  - [10] S. Jeon and L.G. Ya, *Phys. Rev. D* 53, 5799 (1996) [[arXiv:hep-ph/9512263](#)].
  - [11] J.S. Schwinger, *J. Math. Phys.* 2, 407 (1961).
  - [12] L.V. Keldysh, *Zh. Eksp. Teor. Fiz.* 47, 1515 (1964) [*Sov. Phys. JETP* 20, 1018 (1965)].
  - [13] L.P. Kadanoff and G. Baym, *Quantum Statistical Mechanics* (Benjamin, New York, 1962).
  - [14] B. Bezzerides and D.F. Dubois, *Ann. Phys.* 70, 10 (1972).
  - [15] S.P. Li and L.D. McLerran, *Nucl. Phys. B* 214, 417 (1983).
  - [16] P. Danielewicz, *Annals Phys.* 152, 239 (1984).
  - [17] E. Calzetta and B.L. Hu, *Phys. Rev. D* 37, 2878 (1988).
  - [18] St. Mrowczynski and P. Danielewicz, *Nucl. Phys. B* 342, 345 (1990).
  - [19] W. Botermann and R. Maliet, *Phys. Rept.* 198, 115 (1990).
  - [20] St. Mrowczynski and U.W. Heinz, *Annals Phys.* 229, 1 (1994).
  - [21] P.A. Henning, *Phys. Rept.* 253, 235 (1995).
  - [22] D. Boyanovsky, I.D. Lawrie and D.S. Lee, *Phys. Rev. D* 54, 4013 (1996) [[arXiv:hep-ph/9603217](#)].
  - [23] D. Boyanovsky, H.J. de Vega and S.Y. Wang, *Phys. Rev. D* 61, 065006 (2000) [[arXiv:hep-ph/9909369](#)].
  - [24] S.P. Levinsky, A. Ogura and J. Hufner, *Annals Phys.* 261, 37 (1997) [[arXiv:hep-ph/9708263](#)].
  - [25] St. Mrowczynski, *Phys. Rev. D* 56, 2265 (1997) [[arXiv:hep-th/9702022](#)].

- [26] M . E . Carrington, D . f . Hou, A . H achkowski, D . P ickering and J . C . Sow iak, Phys.Rev.D 61, 025011 (2000).
- [27] M . E . Carrington, H . D eñu and R . Kobes, Phys.Rev.D 67, 025021 (2003) [arX iv:hep-ph/0207115].
- [28] B . Bezzerides and P . DuBois, Phys.Rev. 168, 233 (1968).
- [29] P . D anielewicz, Ann.Phys. 197, 154 (1990).
- [30] P . Bozek, Phys.Rev.C 56, 1452 (1997) [arX iv:nuc1-th/9704007].
- [31] Y . B . Ivanov, J . K noll and D . N . Voskresensky, Nucl.Phys.A 672, 313 (2000) [arX iv:nuc1-th/9905028].
- [32] Y . B . Ivanov, J . K noll and D . N . Voskresensky, Phys.Atom . Nucl 66, 1902 (2003) [arX iv:nuc1-th/0303006].
- [33] S . Leupold, Nucl.Phys.A 672, 475 (2000) [arX iv:nuc1-th/9909080].
- [34] S . Leupold, Acta Phys.Hung.New Ser.Heavy Ion Phys. 17, 331 (2003).
- [35] S . Juchem , W . Cassing and C . G reiner, Phys.Rev.D 69, 025006 (2004) [arX iv:hep-ph/0307353].
- [36] S . Juchem , W . Cassing and C . G reiner, arX iv:nuc1-th/0401046.
- [37] S . R . deGroot, W . A . Van Leeuwen and Ch . G . van W eert, Relativistic K inetic Theory (North-Holland, Amsterdam , 1980).
- [38] F . Gelis, Nucl.Phys.B 508, 483 (1997) [arX iv:hep-ph/9701410].
- [39] H . A . Weldon, Phys.Rev.D 28, 2007 (1983).
- [40] S . Jeon and P . J . Ellis, Phys.Rev.D 58, 045013 (1998) [arX iv:hep-ph/9802246].
- [41] S . Jeon, private communication.
- [42] E . M . Lifshitz and L . P . P itaevskii, Physical K inetics (Pergamon Press, Oxford, 1981).
- [43] The different treatment of the  $\phi^3$  and  $\phi^4$  theory comes from the way the coupling constant enters the Lagrangian (1). If we had defined interaction terms of the form  $g^2 \phi^4=4!$  and  $g^3 \phi^3=3!$  we would avoid using the parameter  $\lambda$ .